6271
Sept 11/92

PULSE POSITION MODULATION FOR DISTRIBUTION OF VIDEO SIGNALS ON OPTICAL FIBER

A Thesis

Submitted to the Faculty of Graduate Studies and Research

in Partial Fulfillment of the Requirements

for the Degree of

Master of Science

in the

Department of Electrical Engineering

University of Saskatchewan

by

YOU XING DING

Saskatoon, Saskatchewan

July, 1992

COPYRIGHT

ACKNOWLEDGEMENTS

The author wishes to thank his supervisor Professor D. E. Dodds and Professor S. Kumar for their guidance and encouragement during the course of this work.

Financial assistance was provided by the Natural Science and Engineering Research Council of Canada. Their funding is gratefully acknowledged.

Special thanks are extended to Mr. G. Chin for his discussions and assistance during the course of this work.

Last, but not least, the author gives special thanks to his wife for her patience and encouragement, especially during the last phase of the project.

UNIVERSITY OF SASKATCHEWAN

Electrical Engineering Abstract No. 92A364

PULSE POSITION MODULATION FOR DISTRIBUTION OF VIDEO SIGNALS ON OPTICAL FIBER

Student: Y. F. Ding

Supervisor: Prof. D. E. Dodds
Prof. S. Kumar

M.Sc. Thesis Presented to the
College of Graduate Studies and Research

July 1992

ABSTRACT

Optical fiber distribution networks are being exploited for the provision of video and other wide band services. Digital transmission of these signals is expensive because of the requirement for a complex and costly codec. For short length subscriber links, analog transmission could be preferred for the low cost of the modulator.

This thesis investigates the performance of multichannel video transmission over optical fibers using pulse position modulation (PPM). The performance of PPM is compared to amplitude modulation vestigial sideband (AM-VSB), frequency modulation (FM), and pulse code modulation (PCM), in terms of the demodulated signal-to-noise ratio (SNR) relative to the SNR at the optical receiver. It is shown that PPM SNR performance is comparable to PCM and FM modulation methods. Furthermore, PPM permits some transmission nonlinearity and allows the use of low cost optical transmitters. Integrated services using PPM video signals and multiplexed PCM voice and data signals are also possible.

TABLE OF CONTENTS

COPYRIGHT i

ACKNOWLEDGEMENTS ii

ABSTRACT iii

Table of Contents iv

List of Figures vii

List of Tables x

List of Symbols xi

1. INTRODUCTION 1

2. TRANSMISSION METHODS FOR VIDEO SIGNALS 7

2.1. Baseband Video Signals 7

2.1.1. Division of Amplitude Range 8

2.1.2. Video Signal Frequency 8

2.2. Fiber Optic Communication Systems 10

2.2.1. Optical Transmitter and Receiver 11

2.2.2. System Bandwidth and Attenuation 13

2.3. AM-VSB Multichannel Transmission 15

2.4. FM Multichannel Transmission 17

2.5. PCM Multichannel Transmission 18

3. PULSE POSITION MODULATION 20

3.1. Generation of PPM 20

3.2. Demodulation of PPM 22

3.3. PPM Signal Analyses 23

3.4. Bandwidth Requirements 26

3.5. PPM Multiplexing System 27

4. **SIGNAL-TO-NOISE RATIO PERFORMANCE OF A MULTICHANNEL PPM SYSTEM 30**

4.1. Noise in a Fiber Optical Link 30

4.1.1. Noise Introduced from Optical Transmitter 31

4.1.2. Noise Sources in Optical Receiver 33

4.2. PPM Carrier-to-Noise Ratio (CNR) 37

4.2.1. Definitions of CNR 37

4.2.2. CNR_{tx} at Transmitter........ 38

4.2.3. CNR_{rx} at Receiver 39

4.2.4. CNR_{sys} of the System 41

4.3. Video Signal-to-Noise Ratio (SNR) Standards 41

4.4. SNR Performance of PPM Video Signals 43

5. **COMPARISON OF SNR CHARACTERISTICS 49**

5.1. SNR of AM-VSB Modulated Video Signals 49

5.2. SNR of FM Modulated Video Signals 53

5.3. SNR of PCM Modulated Video Signals 55

5.3.1. Probability of Bit Error in PCM Transmission 55

5.3.2. Quantization Noise 57

5.3.3. SNR Performance of PCM Video Signals 57

5.4. SNR Improvement of PPM Compared with Other formats 59

5.4.1. CNR Requirement and SNR Improvement with Transmission Bandwidth 59

6. **FUNDAMENTAL LIMIT ON NUMBER OF CHANNELS IN OPTICAL VIDEO SYSTEMS 65**

6.1. Intermodulation Distortion 65

6.2. Clipping Distortion 71

6.3. Receiver Sensitivity 73

7. INTEGRATED SERVICES USING PPM AND PCM 77

7.1. PPM and PCM Multiplexing System 77

7.2. Transmission Bandwidth Requirement 79

7.3. Other System Design Considerations 79

8. SUMMARY AND CONCLUSION 82

REFERENCES 85

APPENDIX A. SNR of AM-VSB Video Signals 88

A.1. Definition of CNR and SNR 88

A.2. Relationship Between Carrier Power and
Peak-to-Peak Luminance Signal 88

A.3. Relationship Between RF Noise Power and
Baseband Noise Voltage 89

A.4. Relationship Between CNR and SNR 90

APPENDIX B. SNR of FM Video Signals 92

B.1. Definition of CNR and SNR 92

B.2. Video Signal at the Demodulator Output 92

B.3. Noise Power at the Demodulator Output 93

B.4. SNR of FM Video Signals 96

LIST OF FIGURES

Figure 1.1: Coaxial tree-and-branch system. 2

Figure 1.2: Fiber optic cable Television Transmission System. 5

Figure 2.1: Baseband video signals. 8

Figure 2.2: Picture scanning process. 10

Figure 2.3: Video transmission on an optical fiber with (a) FDM, (b) TDM. 11

Figure 2.4: The typical light-current characteristics of a laser and a LED. 12

Figure 2.5: Typical range of attenuation vs. frequency for optical fiber. 14

Figure 2.6: An AM-VSB Multichannel system. 15

Figure 2.7: Radio Frequency Plan. 16

Figure 2.8: An FM Multichannel system. 17

Figure 2.9: A PCM Multichannel system. 18

Figure 3.1: A waveform in generation of uniform PPM. 21

Figure 3.2: A PPM modulator. 22

Figure 3.3: Demodulation of PPM. 23

Figure 3.4: A PPM demodulator. 24

Figure 3.5: Frequency spectrum of an impulse PPM wave. 25

Figure 3.6: Unmodulated PPM pulses. 26

Figure 3.7: Spectrum of unmodulated PPM signals. 27

Figure 3.8: A PPM Multichannel system. 28

Figure 3.9: Multiplexed PPM signals. 29

Figure 4.1: Light output and noise characteristics of a typical laser. 32

Figure 4.2: Light-current characteristics of typical semiconductor lasers. 33

Figure 4.3: Shot-noise equivalent circuit. 34

Figure 4.4: Thermal-noise equivalent circuit. 34

Figure 4.5: Electrical-noise equivalent circuit. 35

Figure 4.6: Photodetector and preamplifier stage. (a) Simplified circuit diagram. (b) Equivalent circuit for signal and noise analysis. 37

Figure 4.7: CNR and SNR measured points in the optical link. 38

Figure 4.8: Multiplexed raised-cosine waveform. 39

Figure 4.9: Raised cosine PPM pulse and signal plus noise. 44

Figure 4.10: SNR vs CNR for a PPM multichannel system. 46

Figure 4.11: SNR improvement for PPM with spectrum spreading. 47

Figure 5.1: Block diagram of AM system for theoretical analysis. 50

Figure 5.2: The frequency response of a vestigial-sideband filter. 51

Figure 5.3: Standard level of visual carrier. 52

Figure 5.4: The idealized FM receiver. 53

Figure 5.5: The probability density functions with Gaussian-distributed white noise. 56

Figure 5.6: SNR improvement for AM-VSB, FM (ΔF_{max} = 20 MHz), PCM (f_s = 13.5 MHz, bits/s = 8), and PPM (f_s =13.5 MHz, B_t = 75 MHz). 60

Figure 5.7: SNR gain vs transmission bandwidth spreading. 63

Figure 5.8: SNR improvement for same transmission system bandwidth (B_t = 80 MHz). 63

Figure 6.1: Typical light-current of laser with quasi-nonlinear characteristic. 66

Figure 6.2: Two carriers and their modulation products. 67

Figure 6.3: The intermodulation distortion distribution. (a) The second

order products; (b) The third order products. 68

Figure 6.4: The second order distortion vs. bias current. 70

Figure 6.5: Intermodulation distortion vs. frequency. 70

Figure 6.6: Laser clipping distortion. 71

Figure 6.7: The limitation on required power for various signalling formats. 74

Figure 7.1: Multiplexed PPM and PCM system. 77

Figure 7.2: The time delay of an output optical pulse. 79

Figure A.1: Block diagram of an AM-VSB receiver. 87

Figure B.1: Block diagram of a FM receiver. 91

LIST OF TABLES

Table 4.1: SNR relationships. 43

Table 5.1: System parameters for each subcarrier modulation scheme. 61

Table 6.1: Intermodulation product counts. 69

LIST OF SYMBOLS AND ACRONYMS

Symbols

B_n	receiver noise bandwidth
B_t	transmission bandwidth
e	quantizing error
f_c	carrier frequency
f_s	sampling frequency
f_v	video frequency
F	excess noise factor (APD)
G_a	amplifier gain
G_D	current multiplication factor (APD)
i_{an}	noise current of amplifier circuit
I_b	input bias current
I_r	average detector current
i_{sh}	shot noise current
i_{th}	thermal noise
I_{th}	threshold current
$I_{ph}(t)$	photocurrent generated in the external optical receiver
L_o	amplitude of the light signal
$L(t)$	intensity light power
M	number of channels
m_t	time-modulation index
N_o	noise voltage spectral density
P_c	mean-squared carrier power of the ith channel

P_e	error probability
P_n	total noise power at the input of a demodulator
P_{nq}	mean-squared quantization noise power
P_{nb}	mean-squared output bit-error noise power
q	electronic charge
R_d	input resistance of the PPM demodulator
RIN	relative intensity noise
ΔT_{max}	maximum time deviation of PPM pulse position
T_s	sampling period
V_{pp}	peak-to-peak picture amplitude
v_n	mrs noise voltage
Z_{ph}	equivalent impedance of the photodetector
α	scale factor of time to voltage (volt/second)
τ_p	pulse duration
$\delta(t)$	delta function
β_k	phase modulation index
γ	attenuation coefficient of a optical fiber

Acronyms

AM-VSB	amplitude modulation vestigial side-band format
APDs	avalanche photodiodes
CNR	carrier-to-noise ratio
FM	frequency modulation
FDM	frequency division multiplexing
LED	light-emitting diode
PAM	pulse amplitude modulation

PCM	pulse code modulation
PIN	positive-intrinsic-negative
PPM	pulse position modulation
PWM	pulse width modulation
RIN	relative intensity noise
SNR	signal-to-noise ratio
TDM	time division multiplexing

1. INTRODUCTION

During the three-plus decades of its existence, the cable television industry has gradually become a major supplier of a wide range of video and other services. Cable television is today available in the majority of residences in North America.

The original purpose for cable television was to deliver broadcast signals in areas where they were not readily received with an antenna. These systems were called Community Antenna Television (CATV). In the mid-1970s, satellite delivery of signals added more channels than were available from terrestrial broadcasters. While satellites and earth stations were very expensive, the costs could be spread over many cable operators who, in turn, could serve many subscribers. Three categories of signals came into existence:

- "Super stations " that are distributed nationally over satellite and become mini-networks;
- Specialized channels (for news, sports, weather, education, shopping, etc.);
- Movie channels.

The term CATV became obsolete. Cable television became much more than just a community antenna for areas with poor reception. Cable television became a means of getting programming that was otherwise unavailable.

A great majority of coaxial cable television transmission systems in use today employ a trunking approach based on a tree and branch architecture (see Figure 1.1). Television signals received from satellites, terrestrial microwave, terrestrial broadcast, or locally originated are transmitted to subscribers over a CATV system. This facility, which serves to line up all available TV programs into one contiguous band of channels, is commonly called a *system headend.* The combined headend output is the signal feed to an entire metropolitan area. An entire metropolitan area, or a large service area, can be subdivided into smaller areas. Each smaller area has a distribution center which is called *a service hub.* At the subscriber terminal, the television signals are remodulated to an Amplitude Modulation Vestigial Side-Band (AM-VSB) format compatible with television sets in the home today.

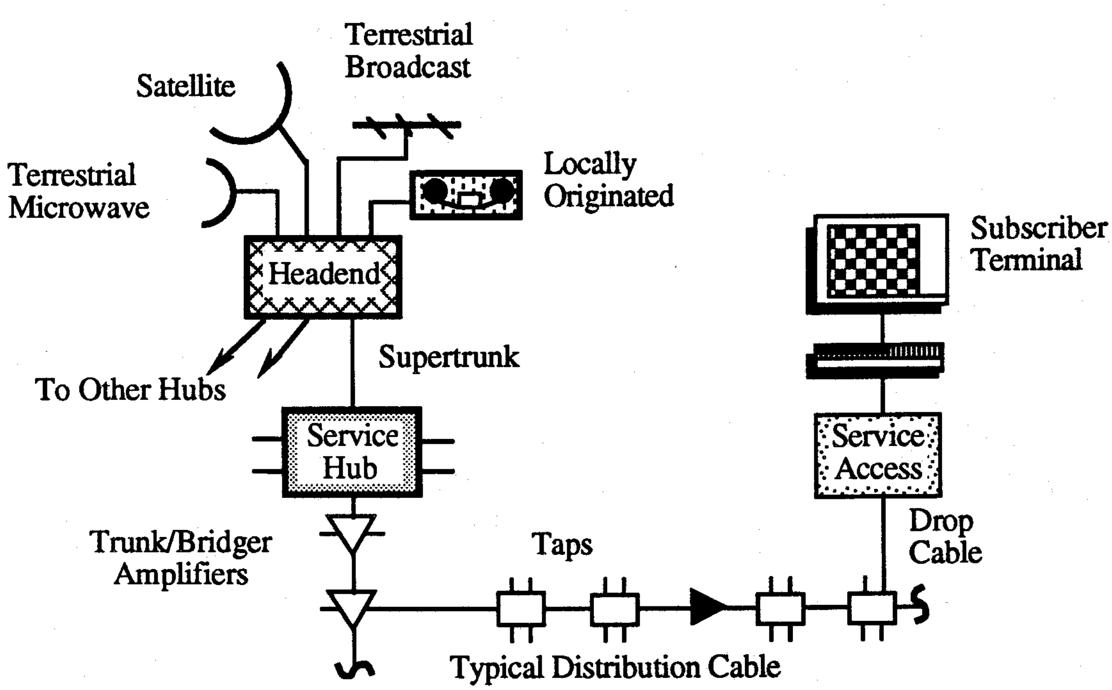

Figure 1.1: Coaxial tree-and-branch system.

It is well known that noise is introduced into television signals which are transported through transmission facilities. Any electrical device, even a simple resistor, will generate some electrical noise within the conducting material due to random electron movements. Cable television systems using radio frequency (RF) carriers require frequent reamplification of the signals because of cable and other transmission losses. Therefore, a relatively large number of cascaded amplifiers must be placed in their transmission paths. Since each amplifier inserted introduces some distortion, the cumulative distortion at the end of a cascade becomes a significant factor in system designs. Such systems could be limited by the distortion in practical applications. It is desirable to find a way to transmit the signals over the same distance while reducing the number of active amplifiers in cascade.

Since its development, optical fiber has been considered as an alternative to coaxial cable for video transmission. Perhaps the most important advantage of fiber over coaxial cable is its low loss. Today's typical single mode optical fiber has an optical power loss that is less than 0.2 dB per kilometer. That means that half the optical power (3 dB) is lost every 7.5 kilometers. This is a dramatic improvement when compared with coaxial cable. For half-inch-diameter aluminum coaxial cable, the attenuation is 30 dB per kilometer. In addition, optical fiber has enormous bandwidth capacity, allowing long haul pulsed transmission of video signals, such as pulse code modulation (PCM) or pulse time modulation. The challenge is to find a way to use those low loss and larger bandwidth characteristics of fiber to make up for current network deficiencies that stem from the high loss and smaller bandwidth of coaxial cable. Figure 1.2 shows a supertrunk cable television transmission system using optical fiber instead of coaxial cable. Because of low loss in optical fiber, video signals can be directly transmitted to subscriber homes from service hubs without repeaters.

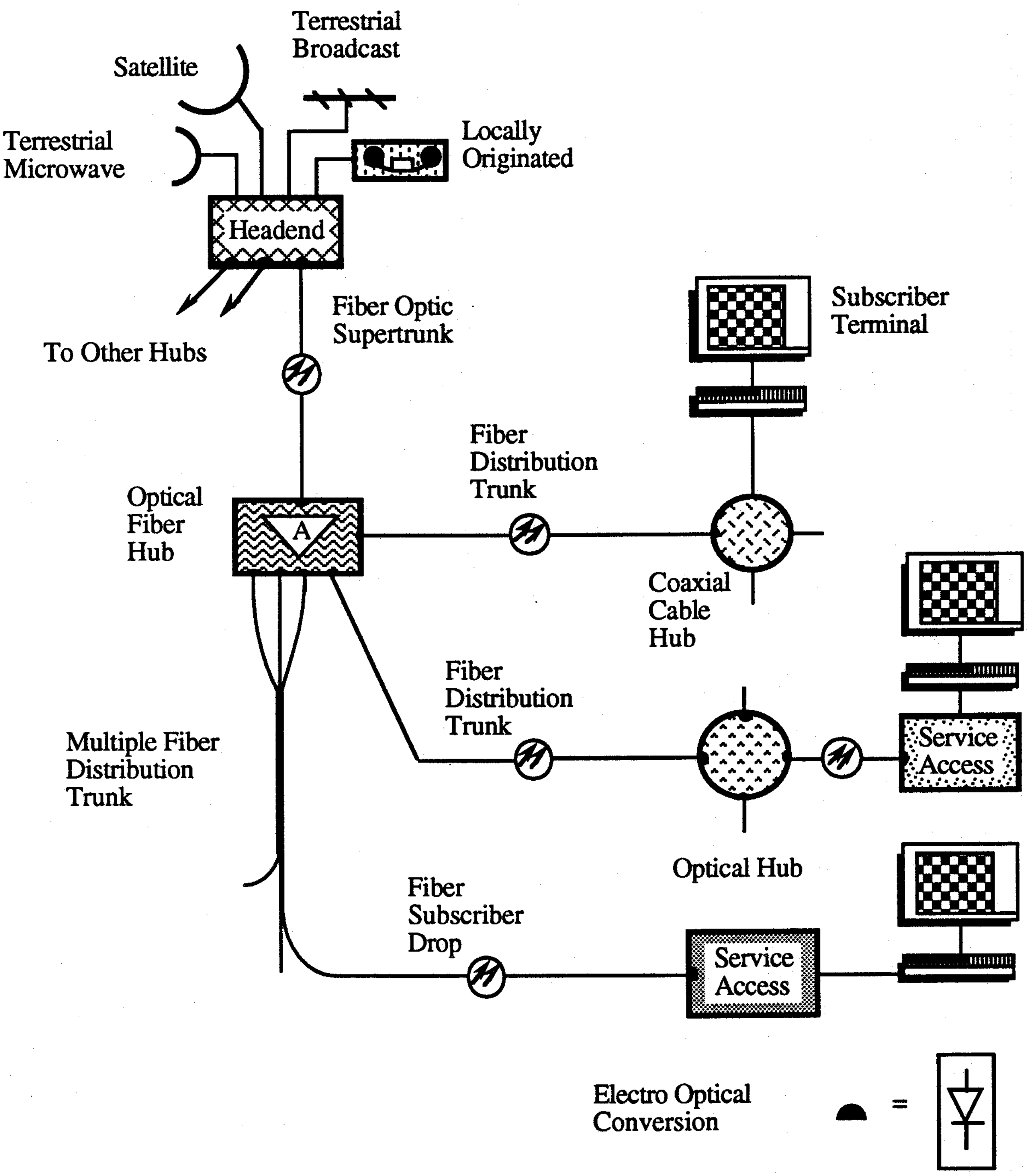

Figure 1.2: Fiber optic cable television transmission system.

Recently, a great deal of research and development effort has been directed towards subcarrier multiplexing over fiber optic supertrunks. Several modulation formats, such as AM-VSB, frequency modulation (FM), and PCM, have been studied or used for the transmission of video information in CATV systems [1-3]. The most obvious is AM-VSB, a highly bandwidth-efficient and practical modulation system for video transmission, which is compatible with existing CATV technology and existing subscriber television sets. Frequency modulation of video signals allows high-quality multichannel video transmission. Digital modulation is an obvious approach to long distance video distribution. Digital modulation has the advantages of offering high transmission quality and almost infinite repeatability, as its binary codes can be recovered and regenerated as needed.

This thesis investigates pulse position modulation (PPM) for multichannel video transmission over optical fibers. PPM is of interest because the problems of laser nonlinearity, clipping distortion, and equipment complexity, have not been fully resolved satisfactorily with the above modulation methods. In PPM, pulses of fixed amplitude and duration are transmitted. The pulses vary in time relative to their unmodulated time of occurrence according to each instantaneous sample of a modulating wave. This relatively simple modulation method requires large transmission bandwidth but permits some nonlinearity in transmission. In the past, PPM has been studied and discarded as a method of voice transmission. It has not yet been studied for video application. The goals of this project were to examine the technical feasibility of PPM for video transmission on a fiber optic link, and to compare its SNR performance with that of other modulation systems.

The following chapter presents several transmission methods for video signals. Chapter 3 describes the basic concept of the generation and demodulation of pulse position modulation. Chapter 4 analyzes the characteristics of PPM carrier-to-noise ratio (CNR) and signal-to-noise ratio (SNR) for video transmission. In order to examine the performance of PPM schemes for multichannel video transmission, the SNR of a PPM system operating under typical parameters is compared to the SNR of other types of modulation formats in Chapter 5. Laser characteristics are discussed in Chapter 6 since laser nonlinearity is a major problem in multichannel systems using analog AM-VSB. Chapter 7 introduces an idea of a multiplexed PPM and PCM systems. And finally, conclusions and recommendations are given in Chapter 8.

2. TRANSMISSION METHODS FOR VIDEO SIGNALS

The modulation formats for video signal transmission can be classified into three categories: (1) analog modulation, such as AM-VSB and FM; (2) digital modulation, such as PCM; and (3) pulse-time modulation, such as pulse position modulation (PPM), pulse width modulation (PWM), and pulse frequency modulation (PFM). Each of these modulation formats has its own system construction for the video signal transmission. The baseband video signal may be directly modulated by any of these modulation techniques with each technique requiring a different transmission bandwidth.

In this chapter, some basic characteristics of baseband video signals and fiber optic communication systems will be described. Then, multichannel video transmission system using AM-VSB, FM, and PCM modulation formats will be briefly introduced.

2.1. Baseband Video Signals

There are several aspects of signal design choices and compromises in existing commercial television systems. The video systems are operated at standard input and output levels terminated by standard load impedances. Television standards vary from country to country. The baseband video signals described here are used in North America and are based on the Electrical Industry Association (EIA-RS-250-B) standards.

2.1.1. Division of Amplitude Range

A typical staircase video waveform [4] is shown in Figure 2.1. The division of video signal levels is defined by the EIA-RS-250-B standard. One portion of the amplitude, from 0 to 100 IRE units, is selected to transmit the brightness information. The highest level is chosen as the value of white and a lower level is chosen as the value of black. The amplitude range between the white and black level is used for transmission of luminance and chrominance signals. The amplitude range between this black level and the minimum level transmitted is available for the transmission of rectangular synchronizing pulses. The signals during this synchronizing time are not visible. The chrominance signal is transmitted by the "color burst", which is a sinusoidal waveform of frequency 3.58 MHz, and peak-to-peak amplitude of 40% of the total luminance signal level (40 IRE units) [4].

2.1.2. Video Signal Frequency

In order to transmit two-dimensional information via a one-dimensional coordinate system, it is necessary to employ some type of *scanning technique*. The image, or picture,

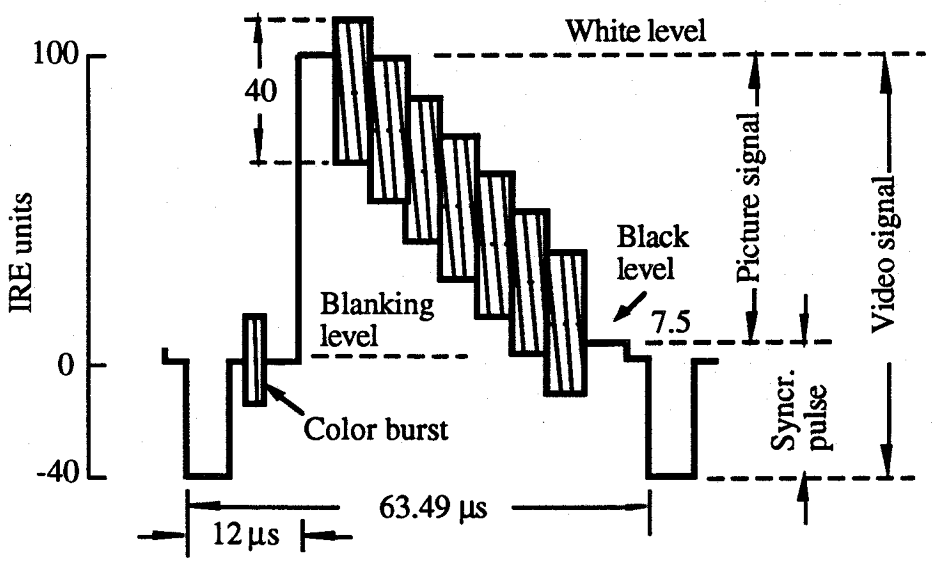

Figure 2.1: Baseband video signals.

can be thought of as a frame subdivided into many small squares, known as pixels (picture elements), defined as a unit of area on the screen. In the North American television system, each frame is divided into 525 horizontal lines [5], of which 485 lines are visible. Each visible line consists of 437 pixels. A frame with 211,945 picture pixels is scanned one line after another. The line pattern used for each frame is called a raster. The relative dimensions of width-to-height are standardized at 4 : 3, and this is known as the aspect ratio.

For transmitting pictures as continuous motion, they must be sent in a fast sequence of at least 40 frames per second in order to eliminate discenible flicker to the human eye. In NTSC systems, only 30 frames per second are sent to save bandwidth. To eliminate the flicker caused by the low frame rate, the 525 lines are scanned in two consecutive patterns. This process is called *interlaced scanning* [5].

A frame is divided into two fields and each field contains 242.5 lines as shown in Figure 2.2. In the first scanning pattern, the entire image is scanned using only 242.5 lines. In the second scanning pattern, the image is scanned again by using 242.5 lines interlaced between lines of the first field. Thus, the effective field rate is 60 fields per second and the frame rate is only 30 frames per second.

As shown in Figure 2.2, a picture is scanned from left to right and top to bottom. Beginning at the upper left, lines 21 up to the first half of line 263 make up the first field. The beam then travels back to the picture top during the vertical retrace period. This is not an instantaneous bottom-to-top jump, but actually requires the length of time equivalent to 20 horizontal lines. These lines are numbered 264 through 283. The second field then begins with the second half of line 283 and ends at line 525. Upon completion of a frame, another vertical retrace, 20 lines, places the beam back at line 21 for the next frame.

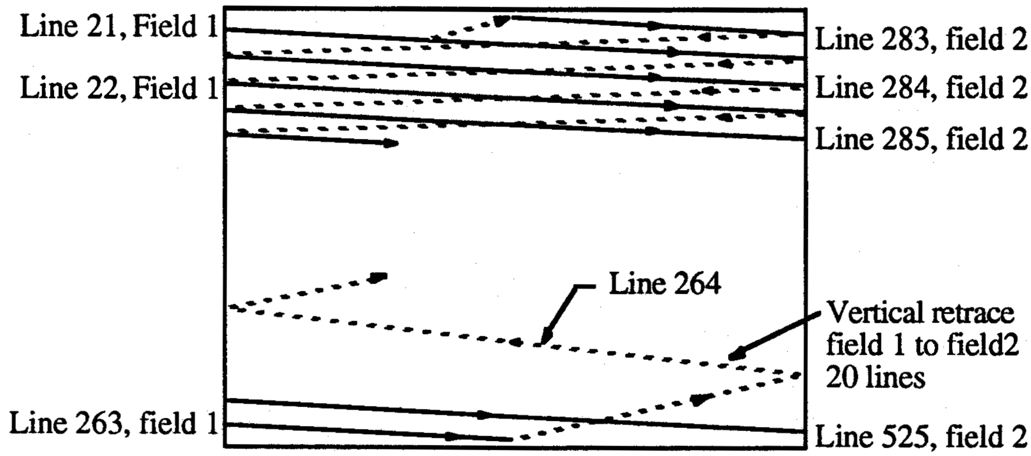

Figure 2.2: Picture scanning process.

At 525 lines/frame and 30 frames/s, 15,750 lines are scanned per second. The reciprocal of 15750 lines/s gives the time per line as 63.49 μs/line. Of this 63.49 μs, 12 μs is used for horizontal retrace from right to left. This leaves 51.49 μs for the visible part of each horizontal line. Dividing by the 437 pixels in a line yields the time per pixel of 0.12 μs/pixel, or 8.3 million pixels/sec. In the worst case, the system would transmit video signals whereby pixels alternate between the darkest and lightest elements 8.2 million times a second. Thus, for video transmission, at least 4.15 MHz of bandwidth is required. A bandwidth of 4.2 MHz is used in practice.

2.2. Fiber Optic Communication Systems

The principal parts of the optical fiber transmission system are transmitter, fiber, and receiver. Each of these parts must handle video signals without distortion with respect to both the intensity and the bandwidth. Multichannel video systems can be realized by using frequency division multiplexing (FDM), in which each channel occupies an allocated frequency range as shown in Figure 2.3 (a). Similarly, as shown in Figure 2.3 (b), with

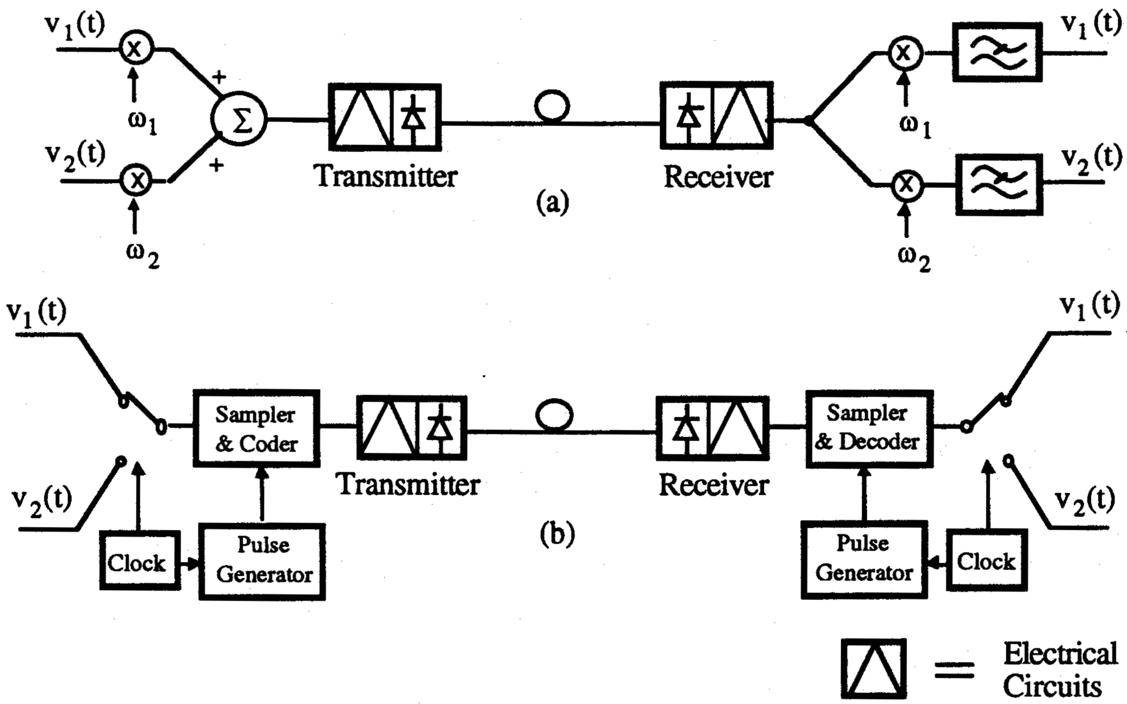

Figure 2.3: Video transmission on an optical fiber with (a) FDM and (b) TDM.

time division multiplexing (TDM), each channel occupies an allowed time slot used for video transmission. Using either technique, system capacity can be further expanded by applying more than one lightwave carrier to a single fiber using wavelength division multiplexing (WDM).

2.2.1. Optical Transmitter and Receiver

Transmitter lasers and light-emitting diodes (LEDs) are in common use as light sources. Typical power-current curves for a laser diode and a LED are drawn in Figure 2.4. Both characteristics show that the current variations of the input electrical signal are converted to proportional optical variations, about an optical current bias, through the laser or the LED. The major considerations in the selection of light transmitters

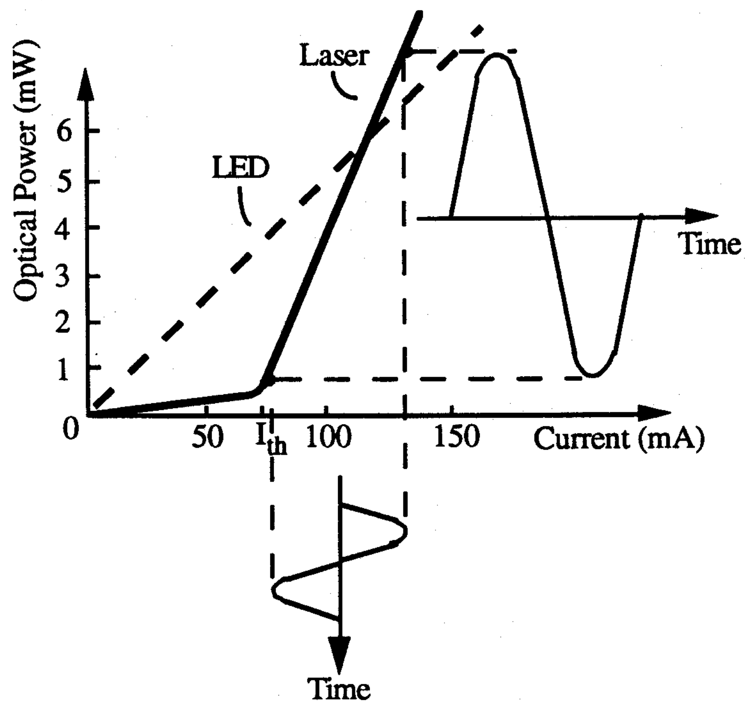

Figure 2.4: The typical light-current characteristics of a laser and a LED.

for cable television application are as follows:

Operating speed. In a digital video multiplexing system, the signal bit rate can be up to tens of gigabits per second. The speed at which a source can operate must satisfy the rise-time requirements of this bit rate.

Power output. The source must couple enough optical power into an optical fiber to overcome fiber and fiber splicing losses. The power level at the input of the detector must still satisfy system signal-to-noise or bit error rate specification.

Peak output wavelength. The wavelength range of 1.3-1.6 μm emitted by the light source is preferred in high quality video transmission because of the low loss in optical fiber (less than 0.2 dB/km) in this wavelength range.

Spectral width. Ideally, a light source should produce a single-wavelength output to eliminate material dispersion in the optical fiber. Most sources emit a number of wavelengths simultaneously.

At the present time, photodetectors are largely limited to positive-intrinsic-negative (PIN) diodes or avalanche photodiodes (APDs). The light emerging from the end of the fiber falls on a photodiode that converts the optical intensity variation to proportional electrical current variations. The major considerations in the selection of optical receivers for cable television application are as follows:

Responsivity. Responsivity is a measure of a detector's output current or output voltage in relation to optical input power. Since responsivity varies with wavelength, it is specified at the wavelength generated by the optical transmitter.

Dark Current. Even in the absence of incident light, some current flows in a photodiods because electron-hole pairs can be generated thermally. Dark current is device temperature dependent.

Response time. The response time of a detector is the time it takes the electrical output to rise from 10 percent to 90 percent of peak output given a step change in received light.

2.2.2. System Bandwidth and Attenuation

Since terminal equipment consists of discrete components, the electrical bandwidth of such components can be defined and measured. The electrical bandwidth is generally defined as the range of video frequencies that may be transmitted through the system and recovered at the distant end. Half-power bandwidth is commonly employed to define system bandwidth. Since -3 dB is a power ratio of 1 to 2, it represents a loss of signal power no greater than 50 percent of the highest signal power within the frequency band.

The optical bandwidth of the fiber, on the other hand, cannot be defined without taking into account the physical length of the fiber. A longer length of fiber will introduce more frequency limitation than a shorter length, so the transmission bandwidth of a specific fiber is a function of the physical length of the facility in which it is employed. For this reason, optical fiber specification must state usable bandwidth in addition to some stated unit of fiber length. Optical fiber bandwidth may be specified in frequency (MHz $\times$ km or GHz $\times$ km). Attenuation, on the other hand, is simply stated as units of loss (dB) per unit of fiber length, usually dB/km. Figure 2.5 shows the attenuation characteristics of optical fiber versus frequency. The low attenuation of 0.15-5 dB/km is uniform over a wide range of modulation frequencies [6].

The bandwidth capacity of optical fiber is in the range of 10 MHz-km to over 1

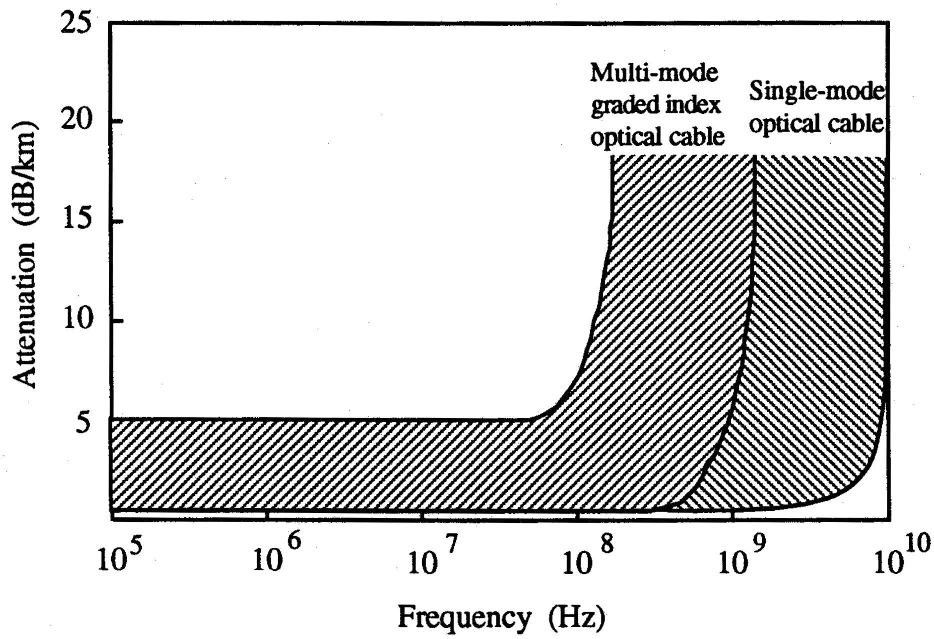

Figure 2.5: Typical range of attenuation vs. frequency for optical fiber [24].

THz-km. Its usable bandwidth with today's terminal devices, however, is roughly equivalent to that of coaxial cable: 1 to 2 GHz. The electrical bandwidth of the transmitter and receiver limits the usable bandwidth on the optical link. While the NTSC television systems operate at a highest frequency of only 300 to 400 MHz, with only the newest systems operating at 550 MHz, one PCM channel with 8-bit picture coding requires a bandwidth of 108 MHz.

2.3. AM-VSB Multichannel Transmission

As mentioned earlier, there are several options available for video signal transmission in cable television systems. One type of modulation commonly used in TV broadcasting is amplitude modulation vestigial side-Band (AM-VSB) format. This format is employed on both coaxial cable systems and fiber optic cable systems today. A block diagram of an AM-VSB multichannel transmission system over a fiber optic link is shown

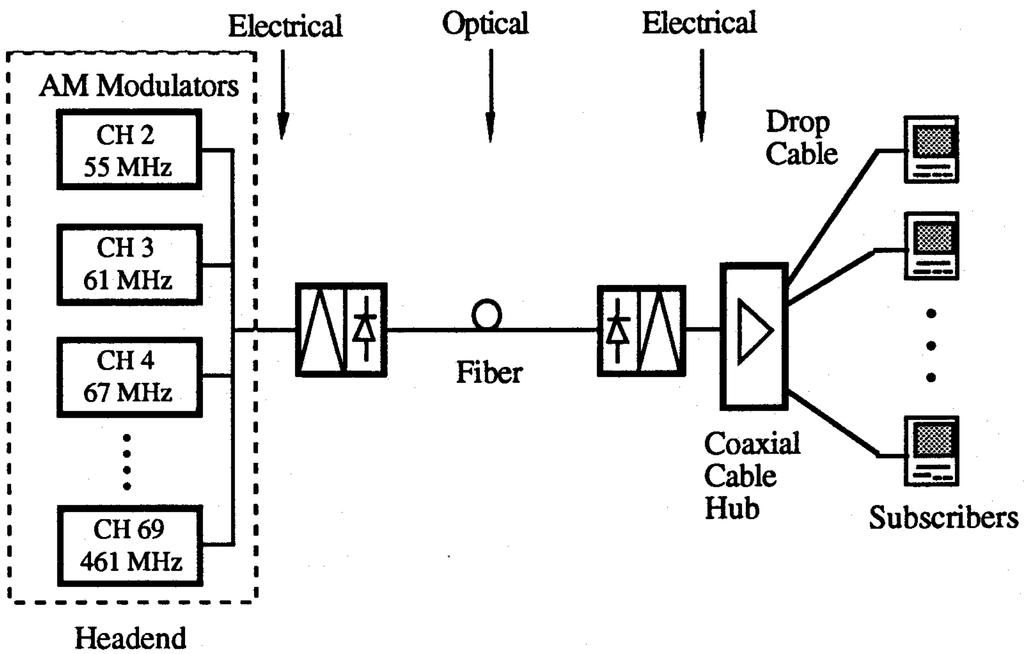

Figure 2.6: An AM-VSB multichannel system.

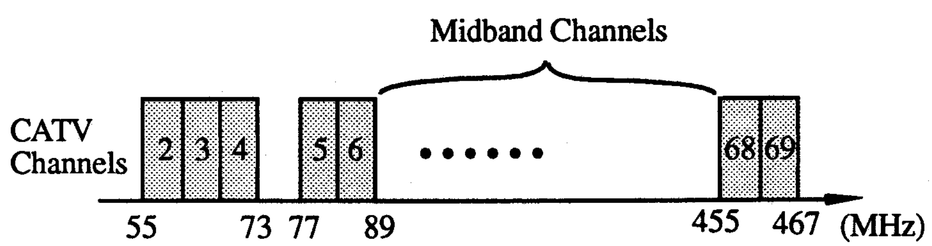

Figure 2.7: Radio frequency plan.

in Figure 2.6. Video signals from different sources are modulated by each individual picture carrier for each video channel. All modulated signals are combined into a broadband signal. An amplitude modulation (AM) fiber link accepts the broadband signal (identical to a headend combined output) as an input and transmits it over a single optical fiber. The other end of the fiber connects with an optoelectronic detector which converts the light modulation back to the broadband electrical signal. The electrical output is compatible with conventional AM on coaxial cable. The following coaxial cable hub, then, transmits the broadband signal to each subscriber.

For AM-VSB, the video signals must be modulated onto carriers in order to deliver multiple signals to subscribers' television sets. Each individual carrier is properly set at its own position in the radio frequency (RF) allocation plan in order to comply with the Federal Communications Commission (FCC) regulation (see Figure 2.7) [7]. In a multiple NTSC system, each AM-VSB video channel is allotted 6 MHz. Whereas double sideband amplitude modulation would need 8.4 MHz, AM-VSB transmits one complete sideband and a vestige of the other in only 6 MHz. Subscribers can select the desired channels by turning their receiver to any 6-MHz portion of the assigned spectrum.

2.4. FM Multichannel Transmission

Frequency modulated (FM) video is widely used for satellite transmission, as well as supertrunking. In an FM system of this type, separation of individual television signals is also achieved by frequency division multiplexing. A multiple FM-system is shown in Figure 2.8. Each video channel must be converted from baseband to an FM modulated signal on an RF carrier. Each channel, with its own carrier, occupies an assigned spectral band. All RF carriers are then combined and multiplexed onto a single optical fiber. The modulation process further expands the spectrum required. FM video requires substantially more bandwidth than AM-VSB video, usually from 10 to 40 MHz/channel, depending upon signal-to-nosie ratio performance. FM performance is discussed in detail in Chapter 5.

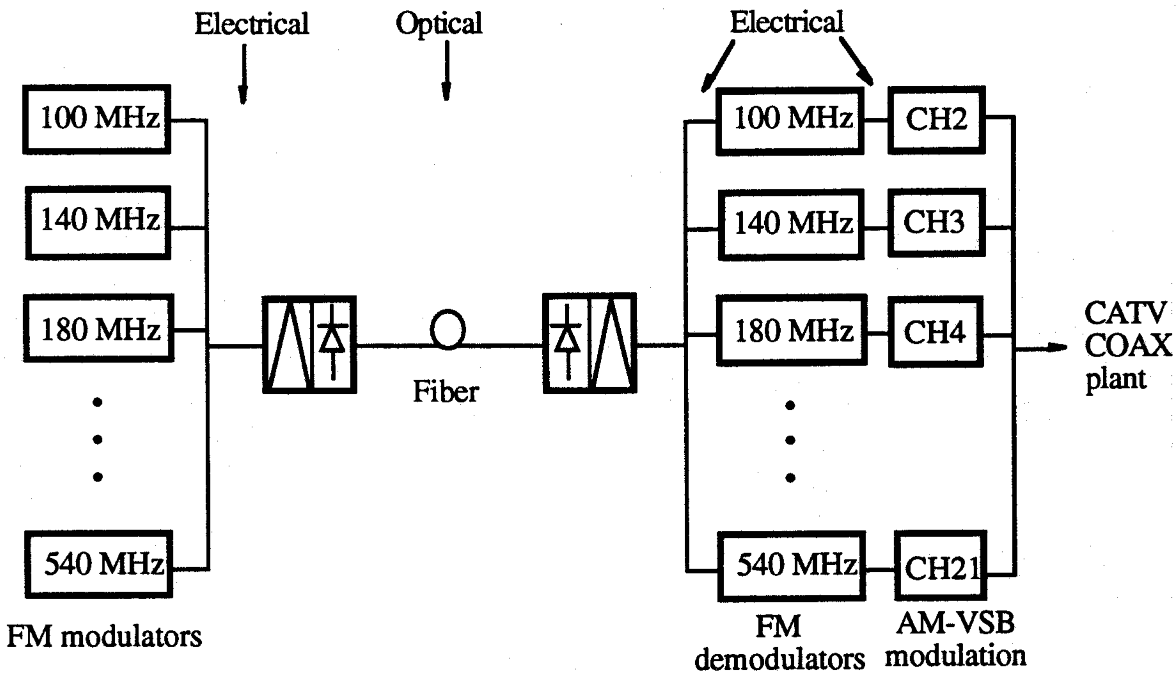

Figure 2.8: An FM multichannel system.

At some point in any FM distribution system, demodulation of the FM signals and AM-VSB remodulation of the resulting baseband video signals are required in order for them to be received by subscribers' television sets. FM has transmission quality advantages over AM, but the costs of modulation conversion limit the extent in which FM can be economically used in practical cable systems.

2.5. PCM Multichannel Transmission

It is possible to digitalize a video signal, and this will probably become the primary method to supertrunk video signals over long distances because of its almost infinite repeatability. Equipment is presently available with pulse cord modulation (PCM) bit rates ranging from 32 Mbps to 108 Mbps for an individual video channel. A typical PCM system for video transmission is shown in Figure 2.9. Analog to digital converters perform the conversion of an analog video signal to a digital video signal. A single PCM video signal can be directly transmitted or a number of PCM video signals can be digitally multiplexed into a pulse stream and sent at a standard hierarchy bit-rate. In North America, the

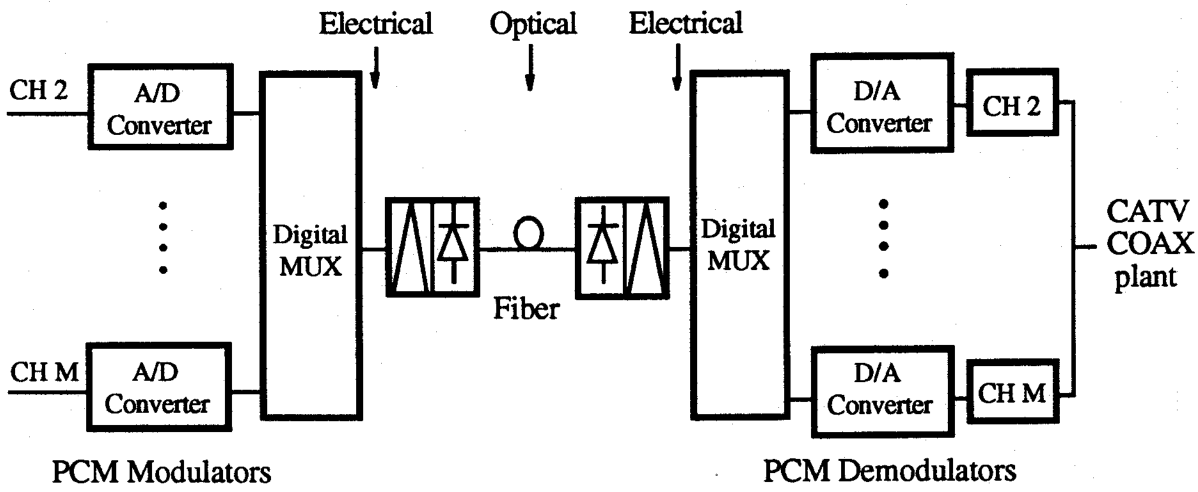

Figure 2.9: A PCM multichannel system.

hierarchy rates [19] for television applications are 44.736 Mbits/s and 139.264 Mbits/s.

Digital terminal devices of this type are still expensive. Costs of devices in digital transmission can be assumed to be directly proportional to bit rate and distance of transmission. An individual A/D and D/A (codec) is required for each channel.

3. PULSE POSITION MODULATION

A great deal of research and development for optical fiber TV distribution networks has been done recently. Most efforts have concentrated on video transmission using analog AM-VSB and FM modulation [1-3]. In this thesis, pulse-analog transmission of video signals on optical fibers using PPM is investigated. PPM is one of several pulse time modulation methods which transmit pulses of fixed amplitude with some parameter varying with time. This modulation method is less complex and somewhat more bandwidth-efficient than PCM. PPM gives the best SNR performance compared with other pulse time modulation methods, such as pulse frequency modulation (PFM) and pulse width modulation (PWM) [8].

3.1. Generation of PPM

The pulse position modulated signal can be obtained from either the uniform sampling or natural sampling methods [19]. In this thesis, only the generation of PPM using uniform sampling is introduced. Waveforms of PPM using a uniform sampling system may be generated as indicated in Figure 3.1. The corresponding block diagram of a practical circuit for generating PPM is shown in Figure 3.2.

The video signal, shown in Figure 3.1(a), is transformed into a pulse amplitude modulated (PAM) signal with instantaneous sampling, utilizing ideal flat-topped rectangular pulses of duration, as shown in Figure 3.1(b). The conversion procedure is achieved by a

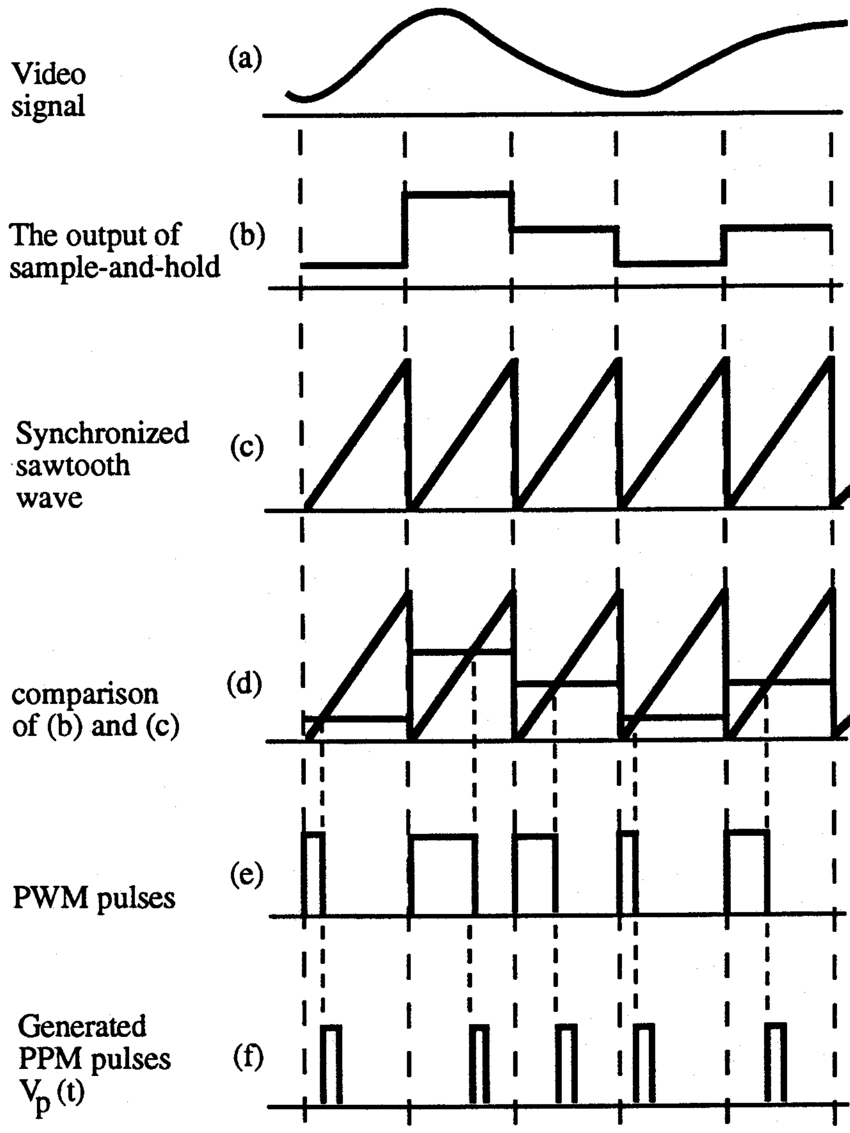

Figure 3.1: A waveform in generation of uniform PPM.

sample-and-hold circuit, which samples the values of the video input that occur at the sampling times and holds them until the next sampling time. A ramp generator produces a ramp waveform extending beyond the amplitude range of the input signal, as shown in Figure 3.1(c). The sawtooth waveform provides the basis for the amplitude-to-timing conversion and therefore must be accurately known. It is resettable by a clock signal.The

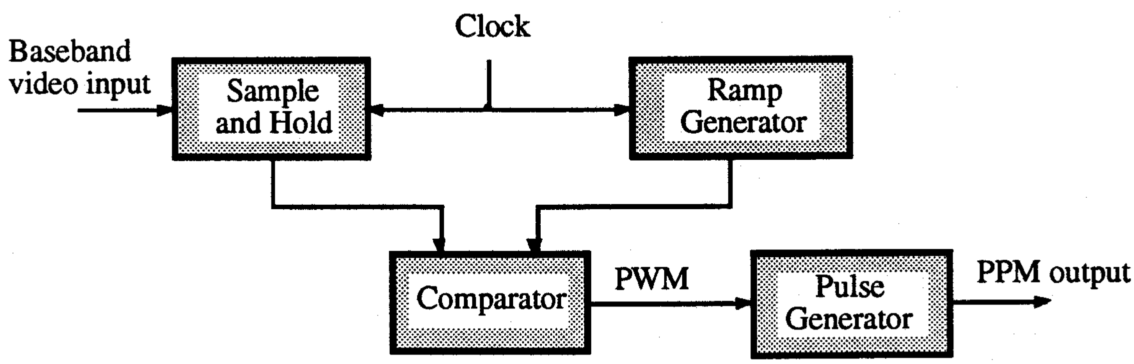

Figure 3.2: A PPM modulator.

PAM signal and the sawtooth wave are directly applied to a comparator, a high-gain amplifier intended for two-state operation. If the sawtooth level is less than the PAM level, the output is held in the high state. Whenever the sawtooth level is greater than the PAM level, the output is held in the low state. A pulse width modulated (PWM) signal, as in Figure 3.1(e), is produced by the comparator. Finally, the PWM pulses trigger a pulse generator with their trailing edges to yield the PPM signal, as shown in Figure 3.1(f).

3.2. Demodulation of PPM

The process of ideal demodulation in PPM consists of conversion to PWM followed by conversion to PAM. The steps are illustrated in Figure 3.3. A block diagram of a practical PPM receiver is shown in Figure 3.4. A train of received PPM pulses is shown in Figure 3.3(a) along with the reference instances. The leading edges of the received PPM pulses reset a PPM to PWM converter, which has been triggered on by a synchronization clock. The output of the converter is a PWM signal, as shown in Figure 3.3(b). The PWM signal is integrated over one sampling period T. The integrated waveform first rises to the level proportional to the duration of the respective PWM pulse. It is then held until the beginning of the successive PWM pulse, at which time the level is dumped to ground on a synchronization clock. The integrated PWM waveform is shown in Figure 3.3 (c). The synchronization signal is supplied by a PPM clock recovery circuit.

A sample-and-hold triggered by the synchronization clock is employed to sample the integrated PWM waveform, as illustrated in Figure 3.3(d). Finally, the PAM signal from the output of the sample-and-hold circuit is passed through a lowpass filter to recover the baseband video signal.

3.3. PPM Signal Analysis

In practice, uniformly-sampled PPM can be generated as illustrated in Figure 3.1, using the system shown in Figure 3.2. Each individual pulse shape is expressed by *p(t)* of

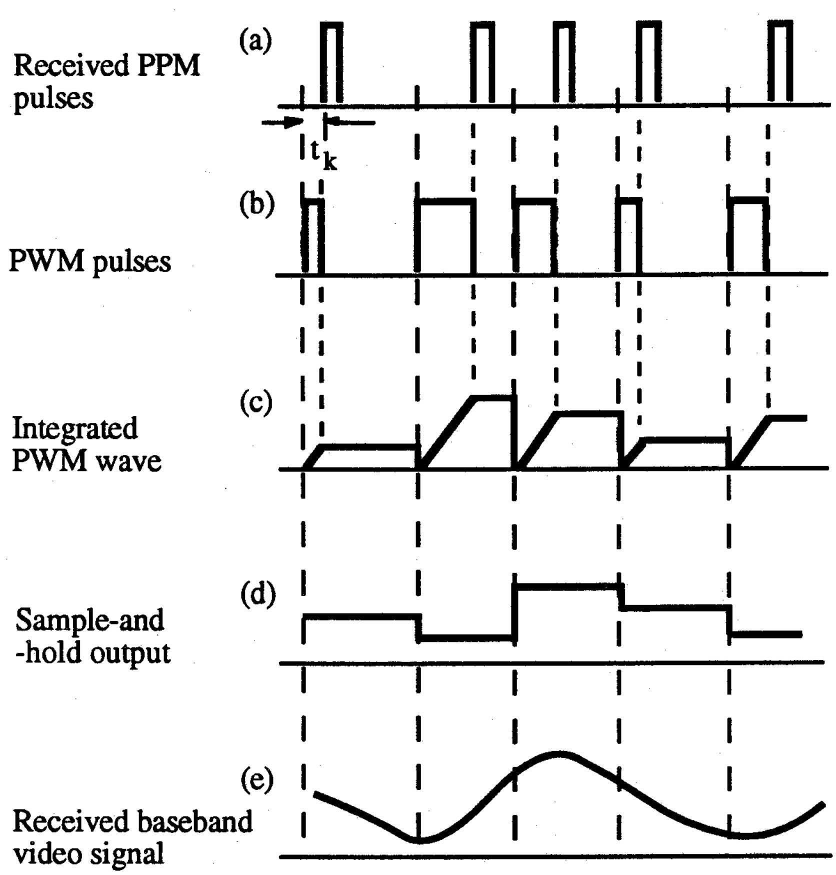

Figure 3.3: Demodulation of PPM.

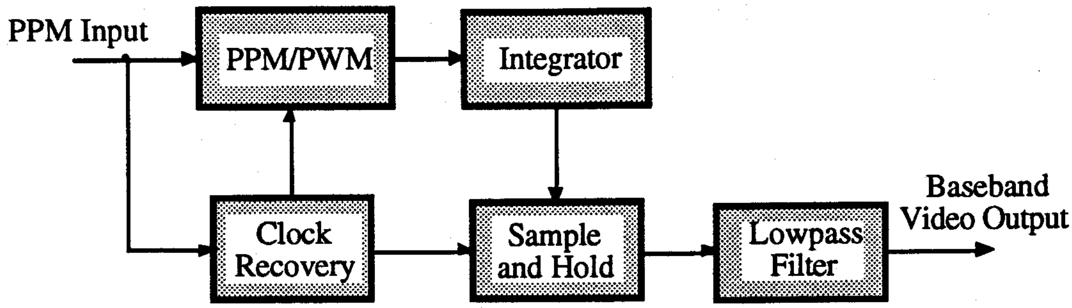

Figure 3.4: A PPM demodulator.

duration τ_p. When not position modulated, the pulse repeats every T_s seconds. The unmodulated train of pulses can thus be considered as a pulse carrier $c(t)$:

$$c(t) = \sum_{k=-\infty}^{\infty} p\,(t - kT_s\,)\ . \tag{3.1}$$

When position modulated, the PPM signal can be described by $v_p(t)$:

$$v_p(t) = \sum_{k=-\infty}^{\infty} p(t - t_k);\ \ t_k = kT_s + m_t\, s_v(kT_s) \tag{3.2}$$

where m_t is the time-modulation index, T_s is the sampling period for video transmission, and $s_v(kT_s)$ is a sample of an input video signal at time kT_s.

The time shift in Equation (3.2) is proportional to the video signal, at kT_s, modified by the scale factor m_t. In order for the pulses in Equation (3.2) to remain within their allotted time slots, the following condition on τ_p must hold:

$$\tau_p \leq T_s - m_t\, s_v\,(kT_s)_{max}\,. \tag{3.3}$$

The PPM wave in Equation 3.2 can be considered as the convolution of $p(t)$, the pulse shape, with a PPM series of delta functions.

$$V_p = p(t) * v_{p\delta}(t)$$

$$v_{p\delta}(t) = \sum_{k=-\infty}^{\infty} \delta(t - t_k); \quad t_{k'} = kT_s + m_t\, s_v(kT_s)\,. \tag{3.4}$$

Using the Fourier series of a train of periodic impulses, the PPM wave of delta functions can be expressed as [9]:

$$v_{p\delta}(t) = \frac{1}{T_s}\left[1 - m_t\, s_v'(kT_s)\right]\left\{1 + 2\sum_{k=-\infty}^{\infty} \cos k\omega_s\big(t - m_t\, s_v(kT_s)\big)\right\}. \tag{3.5}$$

This equation indicates that the impulse PPM wave has an infinite set of sideband images about $\pm kf_s$. The images are amplitude modulated by the derivative of $s_v(t)$ and phase modulated by $s_v(t)$. Furthermore, the phase deviation index of the k^{th} carrier in terms of the phase modulation index β_k is:

$$\beta_k = k\,\omega_s\, m_t\, s_v(t) \tag{3.6}$$

and increases with each integer k.. Thus, the spectra get progressively wider since increased phase deviation results in spectral spreading in the image sidebands. The relative broadening of each successive image is illustrated in Figure 3.5 for the positive portion of the frequency spectrum.

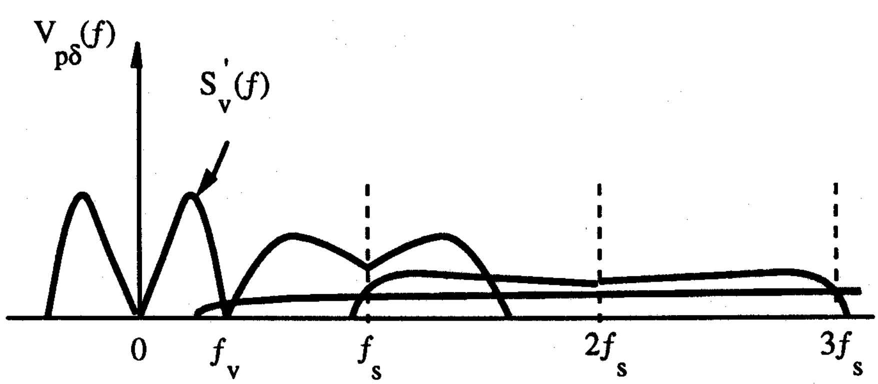

Figure 3.5: Frequency spectrum of an impulse PPM wave [9].

3.4. Bandwidth Requirements

In the preceding section, the interrelated time and frequency domain characteristics of PPM signals are described. This section provides an examination of the effects of pulse duration on transmission bandwidth requirements in PPM.

Consider a train of unmodulated pulses of amplitude A, duration τ_p, and repetition frequency $f_s = 1/T_s$, as shown in Figure 3.6. The exponential Fourier representation of a the unmodulated PPM pulse is given by

$$v_p(t) = \sum_{k=-\infty}^{\infty} P_k \, e^{-j2k\pi f_s t}$$

$$P_k = \frac{1}{T_s} \int_{-T_s/2}^{T_s/2} p(t) \, e^{-j2k\pi f_s t} dt = \frac{A\tau_p}{T_s} \, sinc(2k\pi \, f_s \tau_p/2) \, . \tag{3.7}$$

Equation (3.7) shows that for a fixed sampling frequency, the amplitudes of the frequency components are proportional to τ_p. However, there is an inverse relationship between pulse duration and spectral spreading. A convenient measure of spectral spreading is the bandwidth to the first zero crossing in the P_k function, as shown in Figure 3.7.

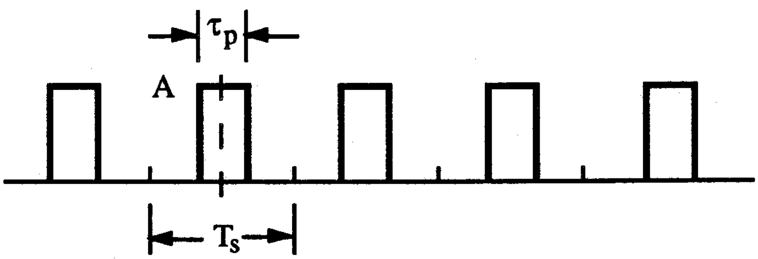

Figure 3.6: Unmodulated PPM pulses.

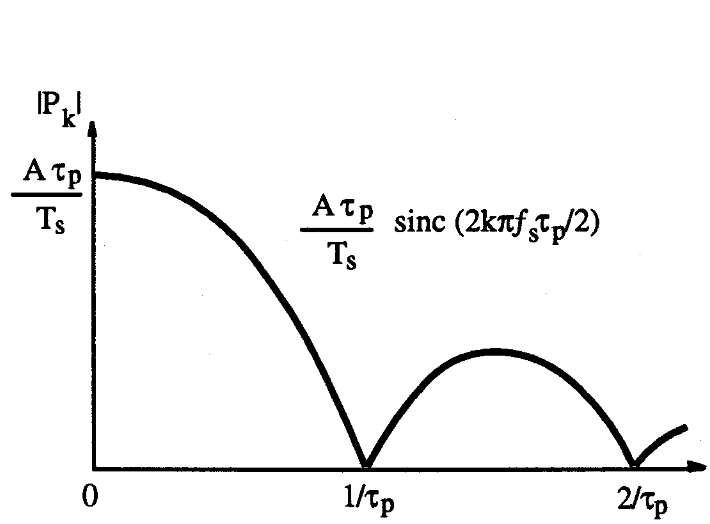

Figure 3.7: Spectrum of unmodulated PPM signals.

For digital communications, the most popular measure of bandwidth is the width of the main spectral lobe, where most of the signal power is contained. This criterion is also suitable for PPM signals. A raised-cosine pulse shape is assumed in this thesis, because its main spectral lobe contains more power than that of a rectangular pulse.

3.5. PPM Multiplexing System

It is clear that several PPM signals may be interleaved in a time-division multiplex system if the pulses are sufficiently short in duration and peak signal modulation is suitably restricted. The different PPM signals may be combined by a multiplexer at the transmitter and separated by a demultiplexer at the receiver. The time multiplexing of M PPM video channels onto a single fiber optic link is illustrated in Figure 3.8. If the pulses are narrow and the peak signal modulations suitably bounded so that different pulses are confined to their respective time slots, each modulating signal can be recovered without distortion and crosstalk.

The M-channel PPM multiplexed signal may be expressed as follows:

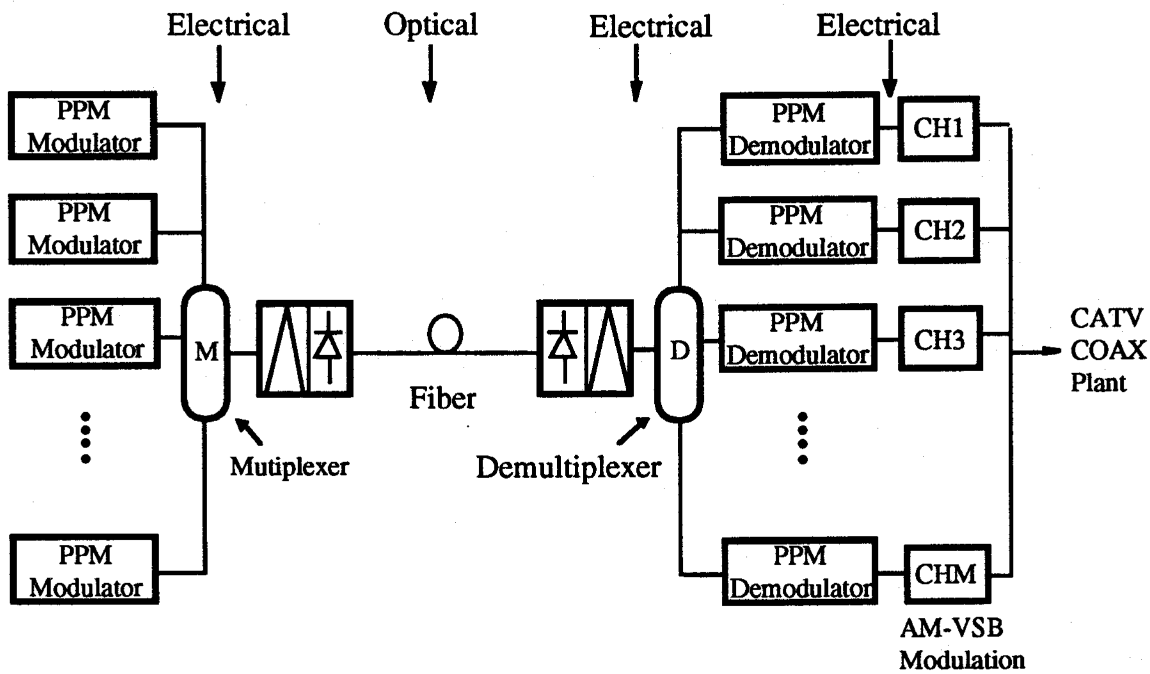

Figure 3.8: A PPM Multichannel system.

$$v_p(t) = \sum_{i=1}^{M} \sum_{k=-\infty}^{\infty} p\left\{t - \left(k + \frac{i}{M}\right) T_s - m_{ti}\, S_{vi}\left[\left(k + \frac{i}{M}\right)T_s\right]\right\} \quad (3.8)$$

This signal consists of M interleaved PPM signals similar to the PPM wave of Equation (3.4). The average duration between pulses is T_S/M. Each of the M video signals $s_{vi}(t)$ is uniformly sampled at a rate $f_S = 1/T_S$. The time multiplexing of M pulse modulated channels within a base time frame T_s is shown as a commutation of the k^{th} sample from each channel in Figure 3.9. The base period T_s corresponds to the sampling period. Each channel is assigned a time slot of duration $T = T_s/M$. The maximum allowable time deviation ΔT_{max} is equal to $m_{ti}\, s_{vi}(t)_{max}$. If the different pulses of $v_p(t)$ are required to be strictly nonoverlapping, the signals must satisfy

$$p(t) = 0, \qquad t \geq \frac{T_s}{M} - m_{ti}\, s_{vi}\,(t)_{max}, \qquad i = 1, 2, ..., M. \qquad (3.9)$$

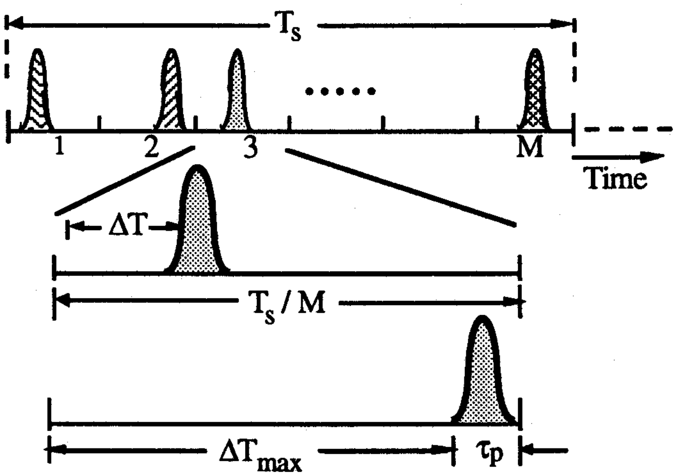

Figure 3.9: Multiplexed PPM signals.

For M video channels, the following criterion must be satisfied to prevent intersymbol interference, or overlap of pulses from adjacent channels:

$$\Delta T_{max} \leq \frac{T_s}{M} - \tau_p . \qquad (3.10)$$

In PPM systems, ΔT_{max} plays an important role because it directly affects signal-to-noise ratio (SNR) performance during demodulation. The SNR improvement is proportional to the amount of time deviation. This is further discussed in the following chapter. The above relationship shows that ΔT_{max} is restricted by the sampling frequency and pulse duration. Thus, either increasing T_s or reducing τ_p can enlarge the time deviation region. Note that the transmission bandwidth will rapidly increase with shorter pulse duration τ_p.

4. SIGNAL-TO-NOISE RATIO PERFORMANCE OF A MULTICHANNEL PPM SYSTEM

The previous chapter introduced the generation and demodulation of pulse position modulation (PPM), as well as PPM signal characteristics. In this chapter, video transmission using pulse position modulation over a fiber optic link will be discussed in detail. To investigate its performance, the PPM demodulation process will be examined under more realistic operating conditions including the presence of noise at the optical transmitter and optical receiver. High quality video transmission requires good signal-to-noise ratio (SNR). The purpose of signal-plus-noise analysis is to show the relationship between the output SNR and the predetection carrier-to-noise ratio (CNR). This relationship exhibits the SNR improvement during the PPM demodulation procedure. In order to analyze SNR and CNR, noise sources in a fiber optic link will be illustrated and described in this chapter.

4.1. Noise in a Fiber Optic Link

Ideally, a device that transmits information provides a unique one-to-one correspondence between input and output signals. In noise free systems with constant frequency response, the output is directly proportional to the input:

$$s_o = k\, s_i \tag{4.1}$$

In practice, there are factors which alter this correspondence. These factors may be treated by assuming the following:

1. The signal is transmitted in an ideal manner.

2. A random signal s_n is added to the transmitted signal before reception:

$$s_o = k\, s_i + s_n \tag{4.2}$$

This random signal is usually referred to as *noise*. In optical images it is frequently referred to as *granularity*. Similar concepts take such names as "*snow*" in television images. When considering noise, there are four main impairments to video transmission in an optical fiber communication system: laser relative intensity noise (RIN), shot noise, thermal noise, and amplifier noise. In this section, these major sources of noise generated in the transmitter and receiver are described.

4.1.1. Noise Introduced from Optical Transmitter

(a) Relative Intensity Noise

At the optical transmitting end, laser diodes display fundamental intensity fluctuation in light output that is called relative intensity noise (RIN). These fluctuations are due to the statistical nature of the carrier recombination process. The intrinsic noise of semiconductor lasers is governed by the quantum processes inside the laser cavity [10] [11]. These processes include shot noise of the injection current, spontaneous recombination of the carriers within the active layer, light absorption and scattering, and stimulated emission. The discrete and random transitions of the excited carriers and the spontaneous stimulated photon emission events are the origin of the basic and unavoidable light intensity fluctuations.

RIN is defined as the total mean-squared noise power per unit bandwidth $\{\Delta l^2\}$ divided by the mean-squared optical output L_0^2 of the laser:

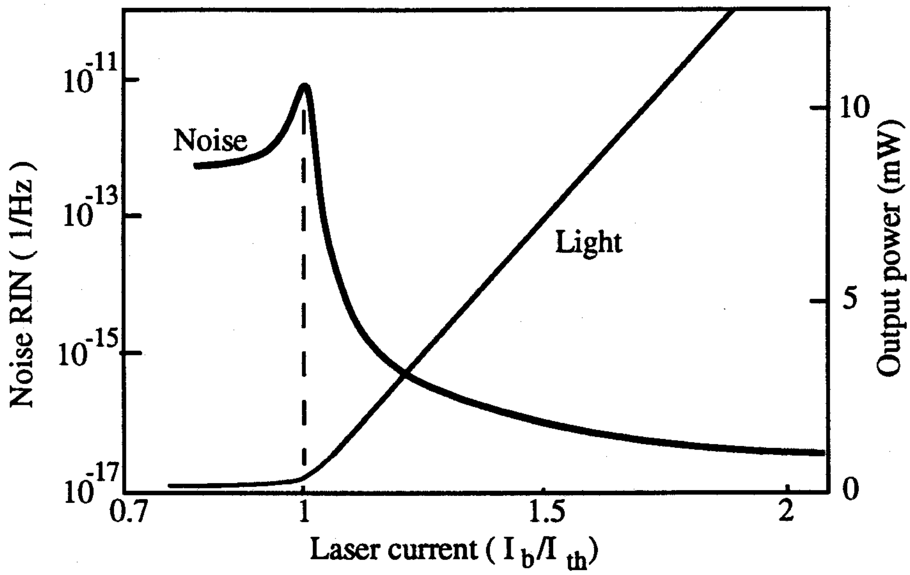

Figure 4.1: Light output and noise characteristics of a typical laser.

$$RIN = \frac{\{ \Delta l^2 \}}{L_o^2} . \tag{4.3}$$

RIN has units of decibels per hertz. A theoretical description of the quantum fluctuations of the lasers has been developed by McCumber [12]. He has shown that the quantum intensity noise attains its peak at the laser oscillation threshold and the noise decreases as the injection current level increases, as shown Figure 4.1. RIN can be approximated as follows:

$$RIN \propto \left(\frac{I_b}{I_{th}} - 1 \right)^{-3} \tag{4.4}$$

where I_b is an input bias current, and I_{th} the threshold current.

Laser noise is a function of its structure and reflections. Lasers are either index-guided or gain-guided as shown in Figure 4.2. Both laser types exhibit a linear light-current characteristic above threshold. However, the transition behavior between the nonlasing and the lasing state is different. The gain-guided laser exhibits a much smoother transition than

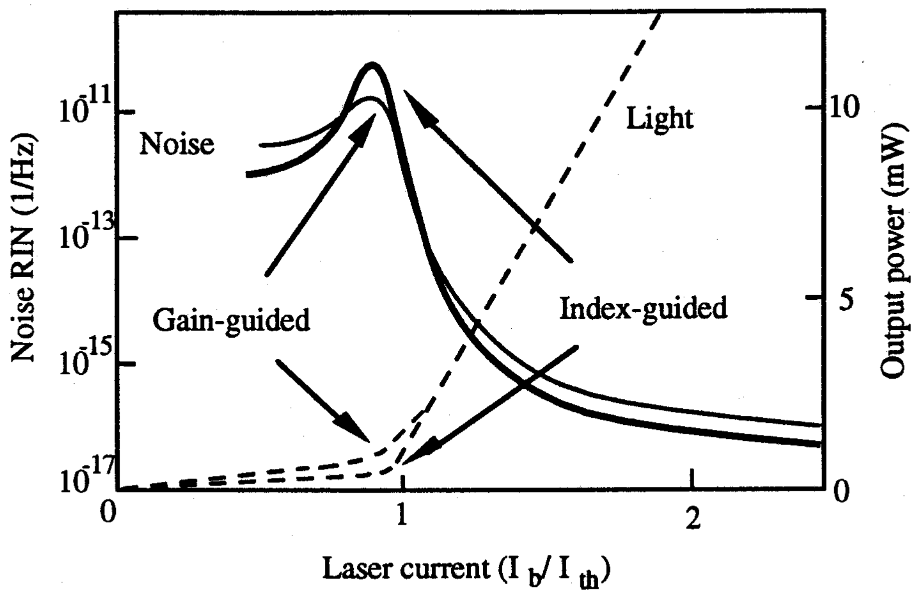

Figure 4.2: Light-current characteristics of typical semiconductor lasers.

the index-guided laser. At the threshold, the noise maximum is inversely related to the smoothness of the light-current characteristics; the smoother the transition from nonlasing to lasing, the lower the noise maximum at the threshold. Experimental results of RIN versus normalized injection current for seven different laser structures are summarized by Sato [13].

4.1.2. Noise Sources in an Optical Receiver

(a) Shot Noise

Shot noise is associated with current flow across a potential barrier. It arises from the fluctuation of current around an average due to random emission of electrons. Shot noise can be represented by an equivalent circuit consisting of a single current source, as drawn in Figure 4.3. The photodetector usually consists of either an APD or a PIN photodiode. Shot noise is present in both types of photodiodes. The PIN photodiode produces the rms shot noise current represented by

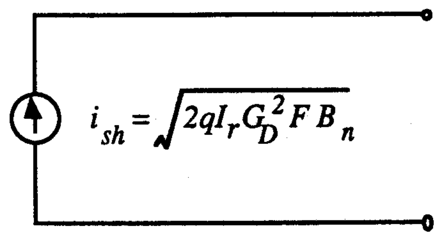

Figure 4.3: Shot-noise equivalent circuit for an APD.

$$i_{sh} = \sqrt{2qI_r B_n} \tag{4.5}$$

where q is the charge on an electron (1.6×10^{-19} C), I_r is the average detector current, and B_n is the receiver noise bandwidth. For an APD, the rms shot noise is

$$i_{sh} = \sqrt{2qI_r G_D^2 FB_n} \tag{4.6}$$

where G_D is the current multiplication factor, and F is the excess noise factor [24]. The shot-noise spectrum is uniformly distributed over all modulation frequencies of interest. This expression represents the effective or rms current. Just like white noise, shot-noise current depends on system bandwidth, and not on the frequency band. According to Equations (4.5) and (4.6), shot noise increases with current. Thus, shot noise is proportional to the incident optical power. This differs from thermal noise, which is independent of the optical power level.

(b) Thermal Noise

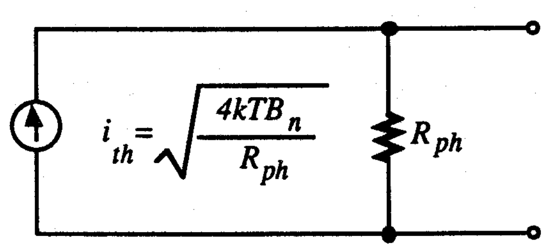

Figure 4.4: Thermal-noise equivalent circuit.

Thermal noise (also called Johnson noise or Nyquist noise) originates within the equivalent resistance of the photodetector R_{ph}. The noise from the resistor is a consequence of the random thermal motions of the charge carriers. These may be observed as a current fluctuation in the resistive component or as the corresponding voltage fluctuation across its terminals. The presence of thermal noise can be modeled by the equivalent circuit drawn in Figure 4.4. In this circuit, R_{ph} is an ideal noiseless resistor. The open-circuit rms noise current produced by the resistance is:

$$i_{th} = \sqrt{\frac{4kT\,B_n}{R_{ph}}} \tag{4.7}$$

where k is Boltzmann's constant, T is the absolute temperature (K), and B_n is the noise bandwidth [24]. Equation (4.7) assumes that the thermal-noise spectrum is uniformly distributed over all frequencies. This is a reasenable assumption up to 10 GHz.

(c) Amplifier Noise

The amplifier is represented by an equivalent circuit having two noise sources i_{an} and v_{an}. The two noise sources can be placed on the input side of the amplifier equivalent circuit, as shown in Figure 4.5. The active device used in the amplifier can be either a bipolar junction transistor (BJT) or a field-effect transistor (FET).

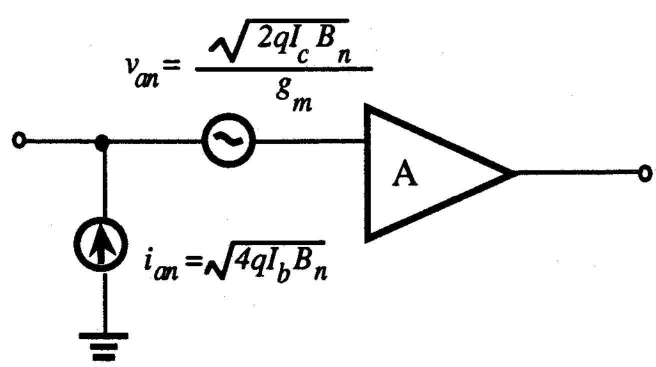

Figure 4.5: Electrical-noise equivalent circuit.

For a first-order, low-frequency approximation, the transistor noise sources can be shot noise with spectral density $2qI$. For the BJT, the spectral densities of the noise current sources are $2qI_b$ between the base and emitter terminals, and $2qI_c$ between the collector and emitter. To refer the collector noise sources to the input side of the transistor, the noise current is divided by g_m. The two noise sources for the BJT amplifier are [24]

$$i_{an} = \sqrt{2qI_b B_n}\ ; \quad and \quad v_{an} = \frac{\sqrt{2qI_c B_n}}{g_m}. \tag{4.8}$$

For a FET amplifier, the corresponding equations are

$$i_{an} = \sqrt{2qI_g B_n}\ ; \quad and \quad v_{an} = \frac{\sqrt{2qI_d B_n}}{g_m}. \tag{4.9}$$

(d) Total Noise in a Receiver

To determine the total noise, a reasonably complete equivalent circuit is examined to identify the noise sources in this circuit. A simplified circuit diagram of the first stage of an optical receiver is shown in Figure 4.6(a). The diagram does not show biasing circuits and other components that have no direct effect on the signals. An equivalent circuit for analyzing signals and noise is shown in Figure 4.6 (b). Using the equivalent circuit in Figure 4.6 and Equations (4.6) to (4.8), an equivalent expression for the total noise referred to the input of the amplifier can be derived:

$$v_n = i_n Z_{ph} + v_{an} \tag{4.10}$$

where

$$i_n = i\sqrt{< i_{sh}^2 > + < i_{th}^2 > + < i_{an}^2 >} \tag{4.11}$$

$$Z_{ph} = \frac{R_{ph}}{1 + j\omega R_{ph} C} \tag{4.12}$$

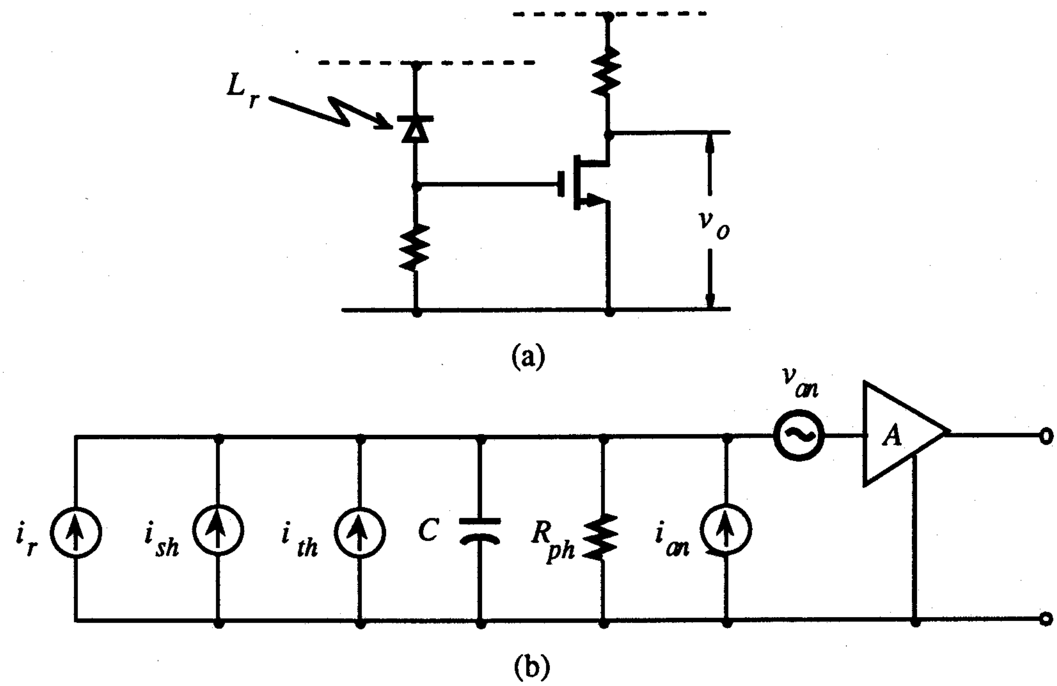

Figure 4.6: Photodetector and preamplifier stage. (a) Simplified circuit diagram. (b) Equivalent circuit for signal and noise analysis.

where the symbol $< x^2 >$ is the mean-asquared value of x., Z_{ph} is the equivalent impedance of the photodetector and C and R_{ph} are the equivalent capacitance and resistance of the photodetector, respectively. The shot noise term, i_{sh}, in Equation (4.11) is applicable to either an APD or PIN photodiode. $G_D = 1$, and $F = 1$ for a PIN photodiode.

4.2. PPM Carrier-to-Noise Ratio (CNR)

4.2.1. Definitions of CNR

The carrier-to-noise ratio of a complete system (CNR_{sys}) may be thought of as the SNR at the input of a PPM demodulator:

$$CNR_{sys} = \frac{\text{received carrier power}}{\text{total noise power}} . \tag{4.13}$$

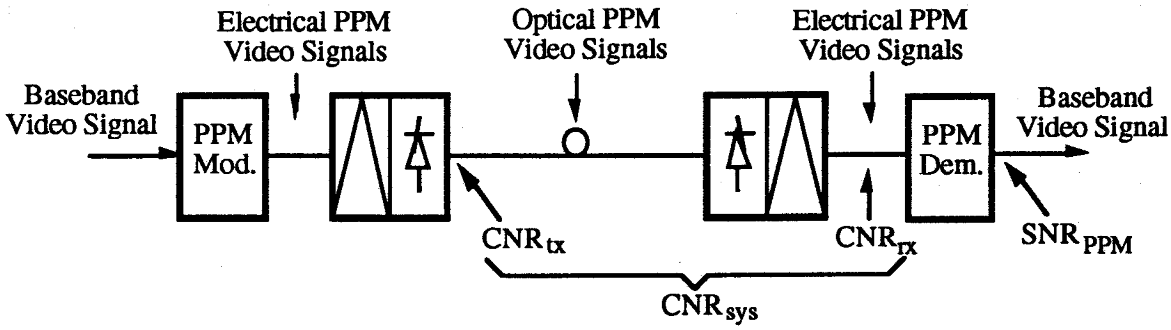

Figure 4.7: CNR and SNR measured points in the optical link.

The carrier-to-noise ratio may also be measured at any point in the transmission link, after the inclusion of significant noise and before filtering. For the system analysis, the carrier-to-noise ratio of the transmitter (CNR_{tx}) and that of the receiver (CNR_{rx}), as illustrated in Figure 4.7, are of interest. Each carrier-to-noise ratio is defined as follows:

$$CNR_{tx} = \frac{\text{transmitted optical power}}{\text{laser noise power}} \tag{4.14}$$

and $$CNR_{rx} = \frac{\text{received carrier power}}{\text{receiver noise power}} \, . \tag{4.15}$$

4.2.2. $\mathbf{CNR_{tx}}$ at the Transmitter

As shown in Figure 4.7, the PPM video signals are applied directly to the light source. The output of the light source can be assumed to retain the same pulse shape as the electrical signal, except possibly a difference in amplitude. The optical pulse can be expressed as:

$$p(t) = L_o \cos^2\left(\frac{\pi \, t}{\tau_p}\right) \qquad \text{for} \qquad -\frac{\tau_p}{2} < t < \frac{\tau_p}{2} \tag{4.16}$$

where L_o is the amplitude of the light signal, and τ_p is the raised-cosine pulse width. Since the PPM pulse deviates ΔT in its allocated time slot of T_s/M in the k^{th} frame (see Figure

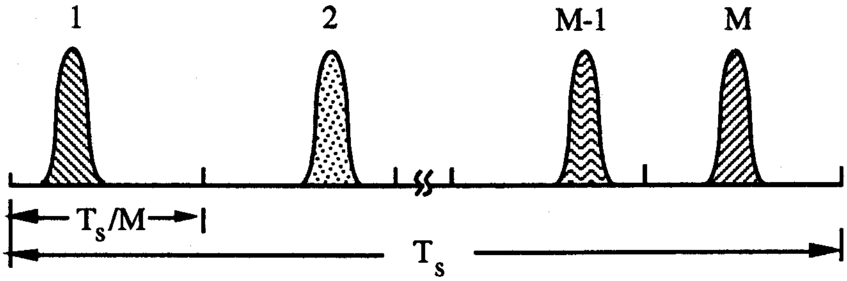

Figure 4.8: Multiplexed raised-cosine waveform.

4.8), the average optical power in one of the individual-channel raised cosine PPM pulses over the sampling time period is given by:

$$L_t = \frac{1}{T_s} \int_{-\tau_\pi/2}^{\tau_\pi/2} \left[L_o \cos^2 \left(\frac{\pi t}{\tau_p} \right) \right]^2 dt = \frac{3\tau_p L_o^2}{8T_s} \, . \tag{4.17}$$

From Equations (4.3), (4.14), and (4.17), the CNR_{tx} may be expressed as:

$$CNR_{tx} = \frac{3\tau_p L_o^2}{8T_s \, B_t \, \{ \Delta l^2 \}} = \frac{3\tau_p}{8T_s \, B_t \, (RIN)} \tag{4.18}$$

where B_t is the transmission bandwidth, and $\{\Delta l^2\}$ is the optical noise density of a laser diode.

4.2.3. CNR$_{rx}$ at Receiver

Received optical power is converted into electrical current by a photodiode in the optical receiver. The conversion procedure consists of the absorption of incident photons in the depletion region, thus creating electron-hole pairs. The photocurrent generated in the external circuit is given by:

$$I_{ph}(t) = \frac{q\eta}{h\nu} L(t) = \rho \, L(t) \tag{4.19}$$

where $L(t)$ is the incident optical power, q is the electron charge, hv is the photon energy, and ρ is the detector responsivity. ρ is related to the quantum efficiency η by:

$$\rho = \frac{q\eta}{hv} . \tag{4.20}$$

The received optical pulse wave at the receiving end may be rewritten to account for the attenuation in the optical fiber:

$$L_r(t) = \gamma\, L_O \cos^2\left(\frac{\pi t}{\tau_p}\right) \tag{4.21}$$

where γ is the attenuation coefficient of the optical fiber. At the output of the photodetector, the received mean-squared power of the i^{th} channel from Equations (4.19) and (4.21) is

$$P_c = \frac{3\tau_p G_a^2 A_r^2}{8T_s R_d}; \qquad A_r = \gamma \rho\, G_D L_o Z_{ph} \tag{4.22}$$

where A_r is the amplitude of the received voltage pulse, G_a is the gain of the amplifier, R_d is the input resistance of the PPM demodulator, and G_D is included to represent APD current amplification. $G_D = 1$ if a PIN is used.

The total noise power at the input of the PPM demodulator may be obtained from Equation (4.10) as follows:

$$P_n = \frac{G_a^2}{R_d}\left[\left(< i_{sh}^2 > + < i_{th}^2 > + < i_{an}^2 >\right) Z_{ph}^2 + < v_{an}^2 >\right]$$

$$= \frac{G_a^2}{R_d} < v_n^2 > \tag{4.23}$$

Thus, using Equations (4.22) and (4.23), the CNR_{rx} is found as in Equation (4.24).

$$CNR_{rx} = \frac{3\ \tau_p\ A_r^{\ 2}}{8T_s < v_n^{\ 2} >} . \tag{4.24}$$

4.2.4. $\mathbf{CNR_{sys}}$ of the System

The relationship between the CNR_{sys}, CNR_{tx} and CNR_{rx} can be developed from Figure 4.7 to be:

$$\frac{1}{CNR_{sys}} = \frac{1}{CNR_{tx}} + \frac{1}{CNR_{rx}} . \tag{4.25}$$

Using the above relationship, and combining Equations (4.18) and (4.24) yields CNR_{sys} as follows:

$$CNR_{sys} = \frac{3\ \tau_p\ A_r^{\ 2}}{8T_s \left[< v_n^{\ 2} > + B_t\, A_r^{\ 2}\ (RIN) \right]} . \tag{4.26}$$

4.3. Video Signal-to-Noise Ratio (SNR) Standards

Since noise is always introduced into modulated signals, it is standard practice in analog communication analysis to measure the degree to which the information has been successfully communicated by determining the output signal-to-noise ratio. There are various definitions of SNR currently employed to define video signal quality. Each definition depends upon what is meant by 'signal' and what is 'noise' and these meanings determine how the measurement is made. These SNR definitions are given as follows [14]:

1. National Cable Television Association (NCTA) standard:

   Signal - the power of the VHF signal during the synch pulse;

   Noise - the noise power in a 4-MHz-wide VHF channel.

2. Television Allocation Study Organization (TASO) standard:

Signal - the power of the VHF signal during the synch pulse;

Noise - the noise power in a 6-MHz-wide VHF channel.

3. Electronic Industries Association (EIA) standard:

Signal - the difference in voltage between the blanking level and the white reference level.

Noise - the r.m.s. noise voltage (nominally between 10 kHz and 5MHz) weighted by the EIA noise weighting network.

4. International Radio Consultative Committee (CCIR) standard:

Signal - the difference in voltage between the blanking level and the white reference level.

Noise - the r.m.s. noise voltage weighted by the CCIR noise weighting network.

5. Bell Telephone Laboratories (BTL) standard:

Signal - the difference in voltage between the synch tip and the reference white.

Noise - the r.m.s. noise voltage weighted by the CCIR noise weighting network.

Within the definitions given above, there are obviously two classes of SNR, i.e., measurements made at VHF and measurements made at video baseband. For NCTA and TASO, the measurement is necessarily made at VHF. Noise power is also read off the meter after the signal is removed. For the latter three standards, the measurements are made at video baseband. A wide-band oscilloscope is used to measure the peak-to-peak voltage at the output of the weighting network. A noise weighting is applied which attempts to take into account the variation in subjective evaluation to interference at various baseband frequencies. In that sense, the latter type of measurements are more nearly a measure of the true quality of the video picture delivered to the customer. The relationship between each standard is shown in Table 4.1 [14].

Table 4.1: SNR relationships.

$SNR_{TASO} = SNR_{NCTA} - 1.8$ dB
$SNR_{EIA} = SNR_{NCTA} + 2.8$ dB
$SNR_{CCIR} = SNR_{NCTA} - 0.2$ dB
$SNR_{BTL} = SNR_{NCTA} + 2.7$ dB

The difference between the EIA and the CCIR is that the EIA applies to color video signals while the CCIR is applicable to black and white signals. In this thesis, EIA standard is employed. The signal-to-noise ratio in EIA-RS-250-B standard for video transmission requires a minimum of 56 dB for satellite TV distribution. This value is assumed as our objective.

4.4 SNR Performance of PPM Video Signals

In PPM, the times of occurrence of the pulses are registered at the receiver by means of a threshold detector. Superimposed noise causes the threshold to be exceeded before or after the instant the pulse value itself crosses the threshold. Displacement of the pulse position by noise in effect inserts noise samples in the receiver output that add directly to the signal samples. Immunity to the effect of noise can be approached by making the pulse build up very steeply so that the time interval during which noise can exert any perturbation is short. The slope of the pulse, however, is limited by the available bandwidth of the transmission medium. As shown later, by increasing the bandwidth it is possible to use short pulses with steeper slopes and thereby improve the signal-to-noise ratio in the output.

With the addition of system noise, the raised cosine pulse and the signal-plus-noise

waveforms are illustrated in Figure 4.9. As shown in the figure, the slicing level for pulse recognition is set at $A_r/2$, which is half the peak pulse height. In the absence of noise, the threshold crossing would occur $\tau_p/4$ prior to the center of the position of the pulse for leading edge triggering. The demodulator in principle converts the time deviation ΔT to the output video-signal amplitude with the scale factor α volt/s. Therefore, the peak-to-peak picture amplitude can be obtained as:

$$V_{pp} = 0.714\ \alpha\ \Delta T_{max} \tag{4.27}$$

However, the deviation from the actual pulse position Δt_n is a random variable, since the addition of the noise v_{nt} at that instant yields a random amplitude. Thus, the squared rms voltage of the output noise is due to the mean-squared position error as in Equation (4.28).

$$V^2_{nrms} = < \alpha^2\, \Delta t_n^2 > = \alpha^2 < \Delta t_n^2 >. \tag{4.28}$$

The relationship between Δt_n and v_{nt} follows from Figure 4.9. The triangle yields the

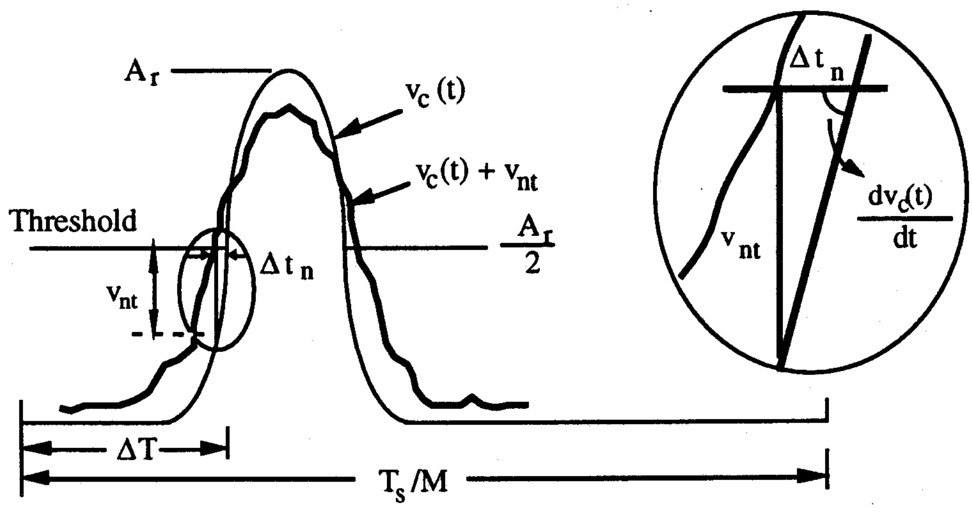

Figure 4.9: Raised cosine PPM pulse and signal plus noise.

identity:

$$\frac{v_{nt}}{\Delta t_n} = \left\{ \frac{d}{dt} \left[A_r \cos^2 \left(\frac{\pi t}{\tau_p} \right) \right] \right\}_{t = \tau_p/4} = \frac{\pi A_r}{\tau_p} \tag{4.29}$$

where v_{nt} is the noise amplitude random variable indexed in continuous time, and A_r is the amplitude of received electrical pulses. Thus, we obtain Equation (4.30):

$$\Delta t_n = \frac{\tau_p v_{nt}}{\pi A_r}. \tag{4.30}$$

Employing Equation (4.30) in Equation (4.28) yields the output noise voltage Equation (4.31).

$$V_{nrms}^2 = \left(\frac{\alpha \tau_p}{\pi A_r} \right)^2 < v_{nt}^2 > \tag{4.31}$$

where

$$< v_{nt}^2 > = < v_n^2 > + B_t A_r^2 (RIN). \tag{4.32}$$

Finally, taking the ratio of Equation (4.27) to Equation (4.31) yields the output SNR for PPM assuming raised-cosine pulses:

$$SNR_{PPM} = \frac{(\ 0.714\ \pi\ \Delta T_{max}\ A_r\ )^2}{\tau_p^2 < v_{nt}^2 >} \ . \tag{4.33}$$

Obviously, SNR_{PPM} increases if the received amplitude of the pulses A_r is increased, thus increasing the signal energy per pulse. Also if ΔT_{max} is increased, due to an increase in the time modulation index m_t, the effect is to have a correspondingly larger signal component added to the sawtooth wave in Figure 3.1. This yields a greater contribution to the deviation of the pulse position. Another factor is the term $1/\tau_p$. It is seen from Equation (4.32) that, as τ_p decreases, SNR_{PPM} increases.

In the multichannel system, the maximum PPM video signal must not cause a pulse to enter adjacent allocated time intervals. Since the slot width is T_s/M, the following criterion must be satisfied:

$$M\left[\Delta T_{max} + \tau_p\right] \leq T_s = \frac{1}{f_s} = \frac{1}{3\ f_v} \tag{4.34}$$

where f_v is the video signal bandwidth. Referring to Figure 3.5, the sidebands about the sampling frequency of an impulse PPM signal are twice the width of the baseband signal. In order to avoid aliasing the sampling rate must therefore be at least three times the highest baseband frequency. This is similar to the Nyquist criteria for natural sampling. As discussed in Chapter 3, the transmission bandwidth can be represented by $B_t \approx 1/\tau_p$. Therefore, ΔT_{max} can then be related to B_t as follows:

$$\Delta T_{max} = \frac{1}{3\ f_v\ M} - \frac{1}{B_t} \tag{4.35}$$

Finally, putting Equation (4.35) in Equation (4.33) gives the per video channel output SNR for PPM, in terms of the ratio of baseband transmission bandwidth to the sampling frequency. The result is

$$SNR_{PPM} = \frac{0.453\, \pi^2 B_t}{f_v} \left(\frac{B_t}{3\, f_v M} - 1 \right)^2 CNR_{sys} . \tag{4.36}$$

The SNR conversion gain characteristics for PPM, with a raised cosine pulse, is plotted in Figure 4.10 as a function of carrier-to-noise ratio (Equation (4.26)). The characteristic is given for the numbers of multichannels, $M = 1, 2$, and 4. In practice, the video baseband is fixed at 4.2 MHz and the transmission bandwidth is considered to be 75 MHz. It is seen that the value of CNR_{PPM} at which deterioration of the SNR_{PPM} (below 56 dB) depends on the number of video channels. When more channels are added to the video transmission

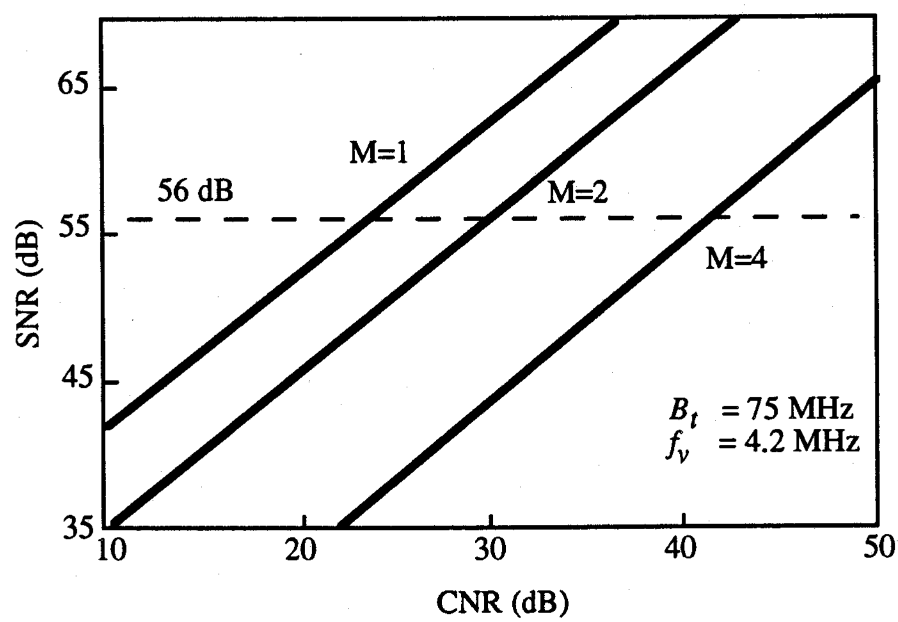

Figure 4.10: SNR vs CNR for a PPM multichannel system.

system, the allowable time deviation of the pulse position becomes smaller, hence reducing SNR_{PPM} performance proportionately.

Because the transmission bandwidth is increased to accommodate a greater time

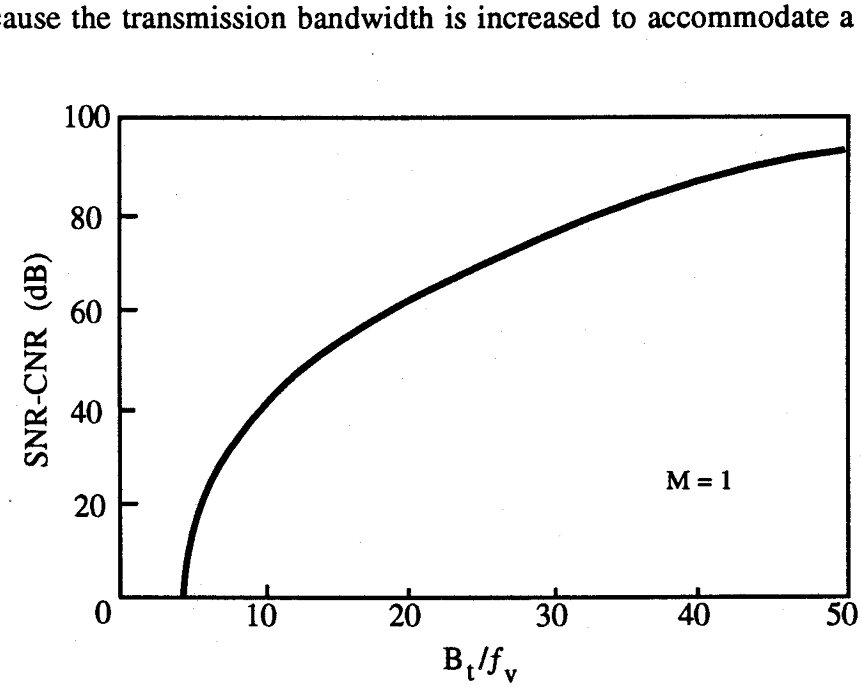

Figure 4.11: SNR improvement for PPM with increasing B_t.

deviation, the SNR gain in PPM increases in proportion to the cube of the ratio of transmission bandwidth B_t, to the video signal bandwidth f_v, when $B_t >> 3f_v$. Figure 4.11 shows that, for $M=1$, SNR improvement is increased with the bandwidth increase of the transmission system. Significant improvement is shown for B_t/f_v between 5 to 20. However, as B_t is increased, the CNR_{sys} must be maintained in order to have the signal dominate the noise achieve the improvement in SNR_{PPM}.

5. COMPARISON OF SNR CHARACTERISTICS

In the PPM SNR analysis shown in the previous chapter, the intrinsic noise and transmission bandwidth of a optical fiber link are two important factors that determine the quality of video signal transmission. Both the intrinsic noise and system bandwidth are characteristic of the transmission medium regardless of the modulation technique employed for the video transmission. The different modulation systems, however, are not equally immune to noise.

As introduced in Chapter 2, analog AM-VSB and FM have been employed for video transmission in existing television networks. For some time, digital PCM has been used for point-to-point video transmission. This chapter focuses on the comparison of SNR improvement in terms of CNR and transmission bandwidth for AM-VSB, FM, PCM, and PPM.

5.1. SNR of AM-VSB Modulated Video Signals

For SNR and CNR analysis on AM optical fiber links, the simplified model in Figure 5.1 of an AM video transmission system is used. In this system, the modulation can generate various amplitude modulation formats, e.g. double-sideband (DSB), single-sideband (SSB), or vestigial-sideband (VSB) signals. A DSB system has an advantage in ease of generation, not requiring sideband suppression. Use of DSB modulation for video transmission would need a frequency allocation of 8 MHz per channel. In contrast, a single-sideband system requires half the bandwidth of DSB system, thus affording good spectrum

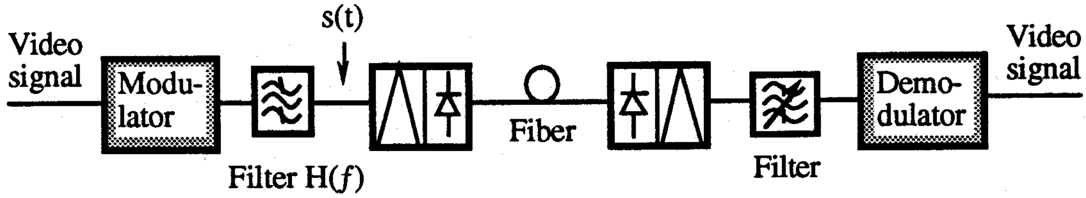

Figure 5.1: Block diagram of AM system for theoretical analysis.

efficiency. However, an ideal filter must completely suppress one sideband without altering the other sideband. In a VSB system, a filter with a gradual cutoff is used. Such a filter is more easily approximated than an ideal filter with a perfectly square pass band, as required for an ideal SSB system.

Vestigial-sideband modulation can be generated by passing a DSB signal through an appropriate filter of transfer function $H(f)$, as in Figure 5.1. The spectrum $S(f)$ of the resulting VSB signal is therefore given by:

$$S(f) = \frac{A_c}{2}[V(f - f_c) + V(f + f_c)]H(f) \tag{5.1}$$

where $V(f)$ is the Fourier transform of the baseband video signal $v(t)$. We wish to determine the specification of the filter transfer function $H(f)$, so that $S(f)$ defines the spectrum of the desired VSB signal. The idealized response of the filter is designed to have an attenuation characteristic over the double-sideband region appropriate to compensate for the two-to-one relationship, as shown in Figure 5.2. This attenuation characteristic is assumed to be in the form of a linear slope over the ± 750 kHz double-sideband region with the crossover located at the midpoint relative to the single-sideband portion of the band [4]. The cutoff portion of this characteristic around f_c exhibits odd symmetry in the sense that inside the transition interval f_c - 750 kHz < f < f_c + 750 kHz, the sum of the values of $|H(f)|$ at two frequencies equally displaced above and below f_c is unity. Such a procedure exactly

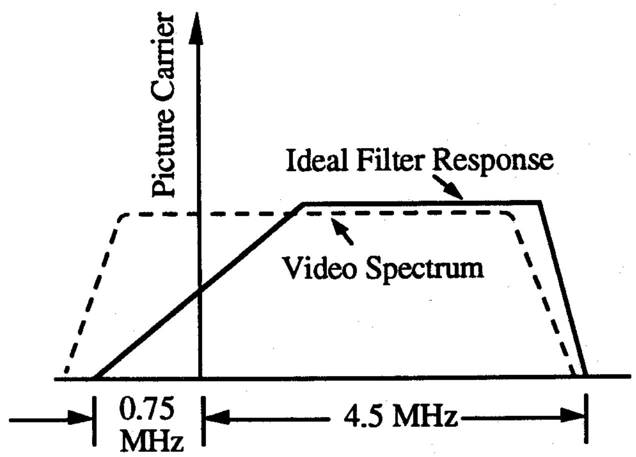

Figure 5.2: The frequency response of a vestigial-sideband filter.

compensates the amplitude response nonsymmetry resulting from the vestigial transmission.

The noise sources in AM optical fiber links may be considered to be the same as those systems described in section 4.1. However, it is necessary to define a bandwidth in which the mean noise power is to be measured at the input of the demodulator. For a standardized measurement, the noise bandwidth is the same as that of the vestigial-sideband receiver filter used for separation of individual video signals. Therefore, the equivalent noise bandwidth, B_n, can be expressed mathematically in terms of the frequency response of the filter, $H(f)$:

$$B_n = \frac{1}{|H_o|^2} \int_0^{\infty} |H(f)|^2 \, df \tag{5.2}$$

where H_o is the maximum absolute value of $H(f)$. Since the mean-squared noise voltage spectral density N_o in an optical link is independent of frequency, the noise power after the filter can be simply expressed as:

$$P_n = \frac{B_n N_o}{R_d} \tag{5.3}$$

where

$$N_O = \left(2qI_r\,F\,G_D^{\,2} + \frac{4kT}{R_{ph}} + 2qI_b\right)Z_{ph} + \frac{2qI_c}{g_m} + A_r^{\,2}\,Z_{ph}^{\,2}\,(RIN)$$

and R_d is the input impedance of the demodulator.

The standard AM-VSB video signals are shown in Figure 5.3 [15]. In North America, a negative standard is used, i.e; less amplitude corresponds to a brighter scene while more amplitude corresponds to a darker scene. The maximum depth of modulation of the visual carrier by the peak-white signal values is specified as 12.5% of the peak carrier level. Also, the black level is transmitted at 75% of the peak carrier level. From inspection of Figure 5.3, the amplitude of the black-to-white transition is only 62.5% of the maximum signal amplitude.

In the EIA-RS-250-B standard [16], the output video signal is defined as the peak-to-peak picture voltage, while the carrier power is considered to be the mean-squared power of the visual carrier during the synchronization pulse. In order to obtain the SNR

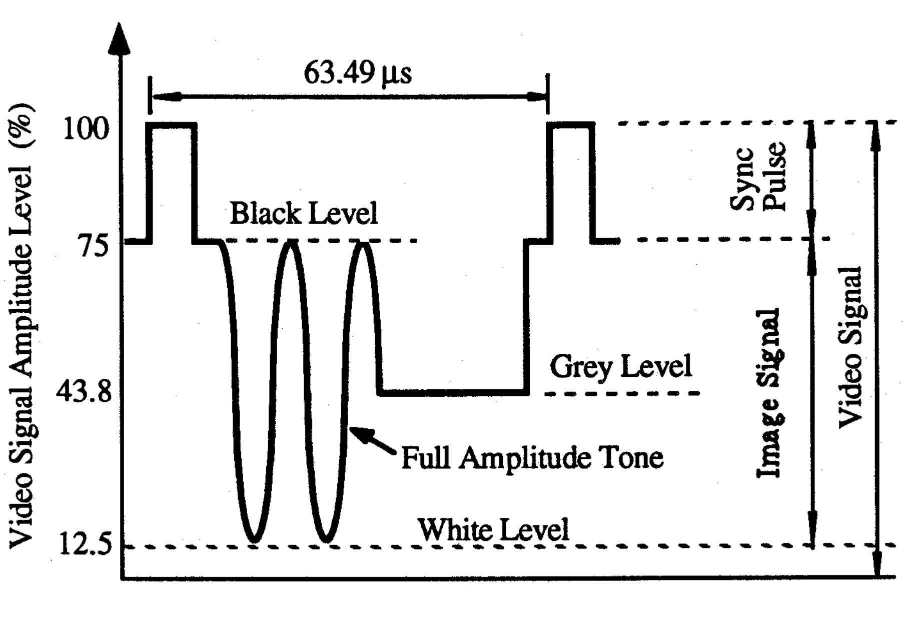

Figure 5.3: Standard levels of visual carrier.

improvement of AM-VSB demodulation, the relationship between the output peak-to-peak picture voltage and the carrier power must be found. It is noted from Figure 5.3 that the carrier component has an amplitude that is 62.5% of the peak synchronization pulses, and the two sideband components each has an amplitude of 15.6%. The relationship between the carrier power and the peak-to-peak picture current may be written as [17]:

$$V_{p\text{-}p} = 0.625\sqrt{2}\,\sqrt{P_c\,R_d} \tag{5.4}$$

where P_c is the electrical carrier power emerging from the filter. From the definition of SNR, we have [see Appendix A]

$$SNR_{AM} \;=\; CNR_{AM}\,(dB) - 1.1\ dB. \tag{5.5}$$

Equation (5.5) shows that the proposed definition makes the 1.1 dB difference between CNR_{AM} and SNR_{AM}.

5.2. SNR of FM Modulated Video Signals

For the purpose of evaluating the effects of bandlimited white noise on the frequency demodulation process, the block diagram of an idealized FM receiver is shown in Figure 5.4. The idealized discriminator output is linearly proportional to the difference between the instantaneous frequency and the carrier frequency. If the peak-to-peak frequency deviation produced by the difference between the white reference levels and the tip of the

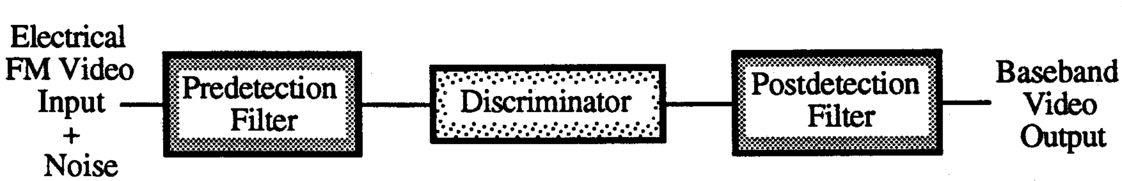

Figure 5.4: The idealized FM receiver.

synchronization pulse is ΔF_{max} , the peak-to-peak picture signal voltage out of the discriminator, according to the standard (see Figure 2.1), is 0.714 ΔF_{max}.

The addition of noise at the discriminator introduces both amplitude noise and phase noise. In the FM case, amplitude limiting is assumed and only phase noise is of interest. Assuming a postdetection filter of known spectral shape $H(f)$ following the discriminator, the mean-squared noise current at the output may be given as [18]:

$$V_n^2 = k_d^2 \frac{B_n^3 N_o}{3P_c} \tag{5.6}$$

where k_d is the modulation index, N_o is the noise power spectral density of the optical fiber link, P_c is the carrier power, and B_n is the equivalent noise bandwidth defined as:

$$B_n = \left[3 \int_0^F f^2 \, |H(f)|^2 \, df \right]^{\frac{1}{3}} \tag{5.7}$$

where F is the cut-off frequency of the postdetection filter. The term f^2 in Equation (5.7) indicats that if a white noise spectral density for the discriminator input is assumed, the output noise spectral density will be parabolic.

Using Equation (5.6), the expression for the peak-to-peak luminance signal, the SNR of the FM format at the receiver output becomes [see appendix B]

$$SNR_{FM} = 12 \frac{(0.714 \, \Delta F_{max})^2}{B_n^3} \frac{P_c}{N_o}. \tag{5.8}$$

With reference to the transmission system bandwidth B_t assumed equal to B_n, Equation (5.8) may be rewritten as:

$$SNR_{FM} = 12\frac{(0.714\Delta F_{max})^2}{B_n^2}(CNR_{FM}) \tag{5.9}$$

where CNR_{FM} is the carrier-to-noise ratio measured at the input of the FM demodulator.

5.3. SNR of PCM Modulated Video Signals

PCM video transmission systems are described in Chapter 2. The first step in changing an analog video signal into a digital form is to convert the video signal into a number of discrete samples. The resulting discrete samples are then coded into discrete code words. Thus instead of transmitting the individual samples at the sample time, a pulse code or pattern is sent at each sample time to convey the information in quantized form. The digitized video signals are decoded back to a number of discrete levels, and then are recovered to baseband video signals at receiver ends. Since the PCM video signal is transmitted in discrete code words, the system performance must be determined by calculating the bit error rate (BER) and quantization noise.

5.3.1. Probability of Bit Error in PCM Transmission

In digital systems, the signal transmitted can be in either of two states, and in the receiver there is a binary-decision process and the probability of error in these binary decisions. In the receiver, the signal plus noise is converted into an electrical signal voltage before the binary decision is made. This voltage is applied to a threshold circuit. If the voltage falls on one side of the threshold voltage, a binary *1* decision is registered; if it falls on the other side, a binary *0* is registered. Because signal levels are not necessarily stable and because the inevitable noise can cause the signal-plus-noise voltage to fall on the wrong side of the threshold, some binary decisions will be in error.

It is assumed that the two discrete levels (A and 0) in the received bit stream are equally probable. The Gaussian distributions representing the two PCM levels are shown in Figure 5.5. The decision threshold can be set at $A/2$ level for minimal probability of error. Figure 5.5 shows that there are instances when $v > A/2$ even though the signal '0' is transmitted. In a similar manner, there are instances when $v < A/2$ with a transmitted '1'. The probability of error, designated by P_{e0} and P_{e1}, is given by the shaded area in Figure 5.5. The net probability of error, P_e, is one-half the sum of the two shaded areas. Finally, it may be expressed by an error function as:

$$P_e = \frac{1}{2} erfc\left(\frac{A}{\sqrt{2P_n}}\right) . \tag{5.10}$$

A is the peak amplitude of a pulse, and P_n is the mean-squared noise power generated in an optical link.

This result can also be represented in terms of carrier-to-noise ratio for the on-off binary case by letting the average carrier signal power per channel equal half the square of the peak pulse amplitude, $P_c = \frac{A^2}{2}$. In a multichannel system, the average carrier power of each individual channel is reduced by the number of channels, M. Equation (5.10) is then rewritten as:

$$P_e = \frac{1}{2}\, erfc\left(\sqrt{\frac{CNR_{PCM}}{M}}\right) \tag{5.11}$$

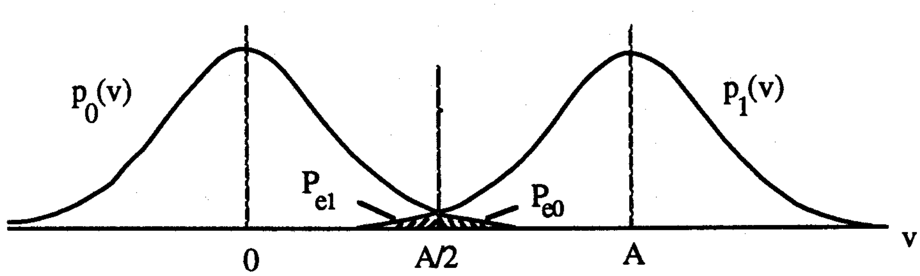

Figure 5.5: The probability density functions with Gaussian-distributed white noise.

where CNR_{PCM} is the carrier-to-noise ratio of one channel.

5.3.2. Quantization Noise

As mentioned earlier, in order to digitize a video signal, the signal is first quantized into a finite number of discrete amplitude levels. The amplitude error between the actual amplitude and the closest discrete amplitude contributes to quantization noise. After quantization, the instantaneous values of the sampled video signal can never be reconstructed exactly. Quantization noise, in contrast to transmission noise, is artificially generated by the quantization process prior to transmission. It can be reduced to any desired degree by increasing the number of the quantizing levels.

To calculate the mean-square quantization noise for a linear PCM system, equal amplitude increments between levels are assumed. The quantizing error e is the difference between the signal level and the nearest quantizing level. If all values of e are assumed to be equally likely anywhere in the range between two levels, the mean-squared quantization noise may be written as [19]:

$$P_{nq} = \int_{-\infty}^{\infty} e^2\, p(e)\, de = \frac{(\Delta A)^2}{12} \tag{5.12}$$

where $p(e)$ is the probability density function of the quantization noise, and ΔA is the amplitude of a quantizing level.

5.3.3. SNR Performance of PCM

The SNR performance of PCM for multiplexed video transmission on a fiber optic link is now examined. For simplicity, the probability of error, P_e, is assumed to be small enough that the probability of more than one bit error in a code word is negligible. In practice, a bit error rate of less than 10^{-9} is required for quality PCM video transmission [3]. Therefore, using a linear quantization rule, an error that occurs in the least significant bit

corresponds to an amplitude error ΔA, and an error in the next higher significant bit corresponds to an error $2\Delta A$, etc. The mean-squared output bit-error noise power per code word arising from optical transmission system is then

$$P_{nb} = P_e \sum_{i=0}^{k} (\Delta A)^2 \, 2^{2i} = P_e \, (\Delta A)^2 \frac{2^{2k} - 1}{3} \tag{5.13}$$

where k is the number of binary digits.

Combining the mean-squared bit-error noise power and the mean-squared quantization noise power, the total rms voltage level can be written as:

$$V_n = \sqrt{(P_{nq} + P_{nb})R_d} \tag{5.14}$$

where R_d is the equivalent impedance of the PCM demodulator.

In linear PCM transmission, video signals are encoded through the entire quantization range, with peak signal excursion of $2^k \Delta A$. According to the EIA-RS-250-B standard, peak luminance is 71.4% of peak amplitude. Therefore, the peak excursion of digitized luminance signal is approximately $0.714 \, 2^k \Delta A$, where the number of quantization levels, k, is equal to or greater than 8. Combining Equation (5.11) and (5.13), the peak signal-to-noise ratio of PCM video signals becomes:

$$SNR_{FM} = \frac{V_{p\text{-}p}^2}{V_n^2} = \frac{(0.714 \times 2^k \Delta A)^2 R_d}{\left(\sqrt{(P_{nq} + P_{nb})R_d}\right)^2}$$

$$= \frac{3 \times 0.714^2 \times 2^{2(k+1)}}{1 + 2(2^{2k} - 1)\ erfc\left(\sqrt{\frac{CNR_{PCM}}{M}}\right)} \tag{5.15}$$

where R_d is the input impedance of the demodulator.

5.4. SNR Improvement of PPM Compared with Other Formats

In previous sections, system performance of each modulation method was determined by calculating signal-to-noise ratio. In practice, the SNR performance of each modulation method presents the efficiency in suppressing noise relative to the signal. With this basic concept as an introduction, the comparative SNR properties of a representative group of AM-VSB, FM, PCM, and PPM systems are discussed.

5.4.1. CNR Requirement and SNR Improvement with Transmission Bandwidth

According to the EIA-RS-250-B standard [16], 56 dB SNR is required for satellite video transmission. In Figure 5.6, the SNR of the received video channels is plotted against the total CNR objective for standard NTSC AM-VSB, FM, PCM, and PPM. The system parameters for each modulation scheme for a 56 dB SNR requirement are listed in Table 5.1.

The SNR_{AM} of the AM NTSC scheme is known to be 1.1 dB less than the CNR_{AM} from Equation (5.5). As can be seen in Figure 5.6, therefore, the AM-VSB systems with high CNR_{AM} requirement need extremely large signal levels relative to the noise level to produce high quality reception. Consequently, these systems suffer from intermodulation distortion (IMD) because of the nonlinear characteristics of lasers. The IMD increases with carrier power and the number of video channels due to the increase of the second and third order distortion products, which are further discussed in the next chapter. Therefore, the modulation index must be low for each video channel. Poor receiver sensitivity resulting from low SNR improvement demands low attenuation in a subcarrier multiplexing (SCM) video distribution network.

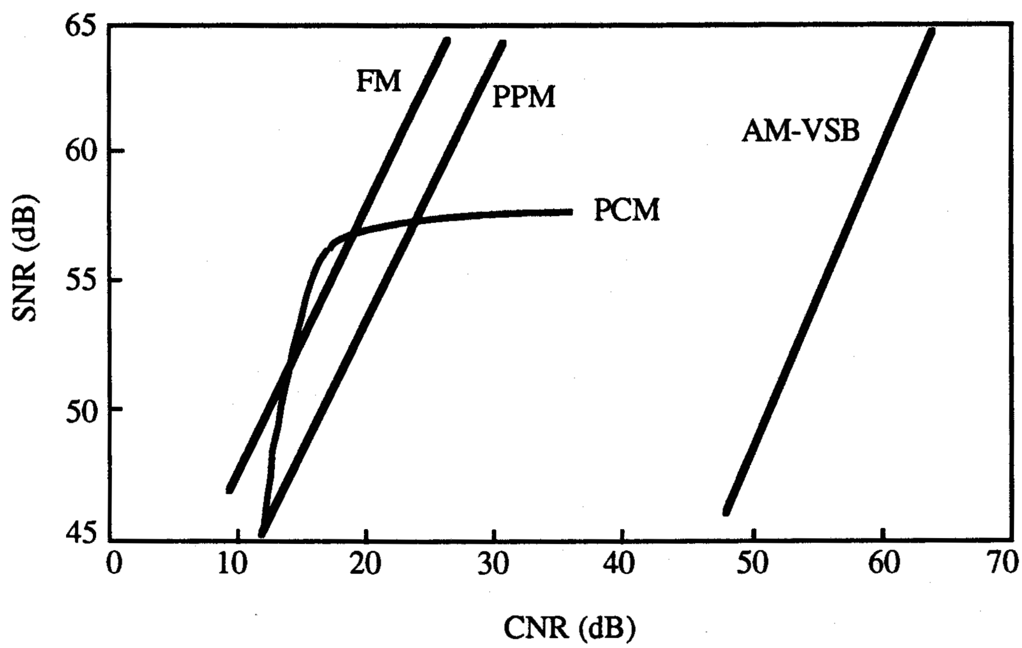

Figure 5.6: SNR improvement for AM-VSB, FM (ΔF_{max} = *20 MHz*), PCM (f_s = *13.5 MHz*, Bits/s = 8), and PPM (f_s = *13.5 MHz*, B_t = *75 MHz*).

Table 5.1: System parameters for each subcarrier modulation scheme.

Modulation Formats	Single Channel		50 Channels			
	CNR dB	BW MHz	Channel Spacing MHz	Sampling Rate MHz	System BW GHz	Demodulator Cost
AM-VSB	56	4.2	6	-	0.3	Low
FM	17.2	30	40	-	2	Medium
PCM	17	108	-	13.5	5.4	High
PPM	23.11	75	-	13.5	3.75	Medium

However, AM-VSB is attractive because of high channel capacity. A multichannel AM video distribution system with 6 MHz allocated to each channel may require only a few hundred megahertz of transmission bandwidth for frequency division multiplexing. For example, 50 AM-VSB video channels can be transmitted in a 300 MHz band, as shown in Table 5.1. Low cost electronics and compatibility with currently installed CATV (Community Antenna Television) customer premise equipment are also attractive factors.

Analog FM with 20 MHz frequency deviation has a CNR_{FM} requirement of 17.2 dB to meet the needed video SNR_{FM} objective of 56 dB as shown in Figure 5.6. From Equation (5.8), a significant improvement in SNR_{FM} can be achieved if an increase in required transmission bandwidth is allowed. Therefore, in FM systems, an increase in transmission bandwidth provides a proportional increase in output SNR_{FM}.

However, if all system parameters are kept fixed, while the frequency deviation, and hence, required transmission bandwidth increases, more noise is accepted by the optical receiver. Eventually, the noise power at the receiver becomes comparable to the signal power. In this case the SNR_{FM} improvement with bandwidth, which assumes large CNR_{FM}, does not hold. In practical video transmission systems, FM video signals consume 26-32 MHz of bandwidth per channel, and typical spacing is 40 MHz. Table 5.1 shows a 2 GHz bandwidth requirement for the transmission of 50 video channels using FM.

It is obvious from Equation (5.15) that SNR_{PCM} is proportional to the number of bits per sample and the predetected CNR_{PCM}. When the CNR_{PCM} is increased, i.e., reducing bit error rate, the SNR performance is, at first, improved very rapidly. It is also noted from Figure 5.6 that, when the number of bits per sample is fixed, the SNR_{PCM} cannot be improved beyond a certain level by increasing CNR_{PCM}. Under this condition, the quantization noise is the primary factor in the SNR_{PCM} performance. In this case, the SNR can be improved only by increasing the number of bits per sample. The SNR_{PCM} of PCM video increases about 6 dB for each additional bit used. However, because required transmission bandwidth is proportional to bit rate, the more bits used per sample means more bandwidth is required.

If eight-bit coding is assumed in Equation (5.14), 56.5 dB is the maximum SNR_{PCM}. This figure just meets the requirement of 56 dB. Therefore, in some digital video transmission systems, eight bits is accepted for picture coding [20]. The sampling frequency is usually set to 3 or 4 times the video color subcarrier frequency. In Table 5.1, a 108 MHz transmission bandwidth is required for a PCM system with 13.5 MHz sampling frequency and eight-bit coding.

For PPM, the SNR_{PPM} improvement is proportional to the ratio of transmission bandwidth to maximum video frequency. Figure 5.7 shows a SNR_{PPM} improvement of 32.92 dB for a 75 MHz system bandwidth. Equation (4.35) exhibits that a SNR_{PPM}

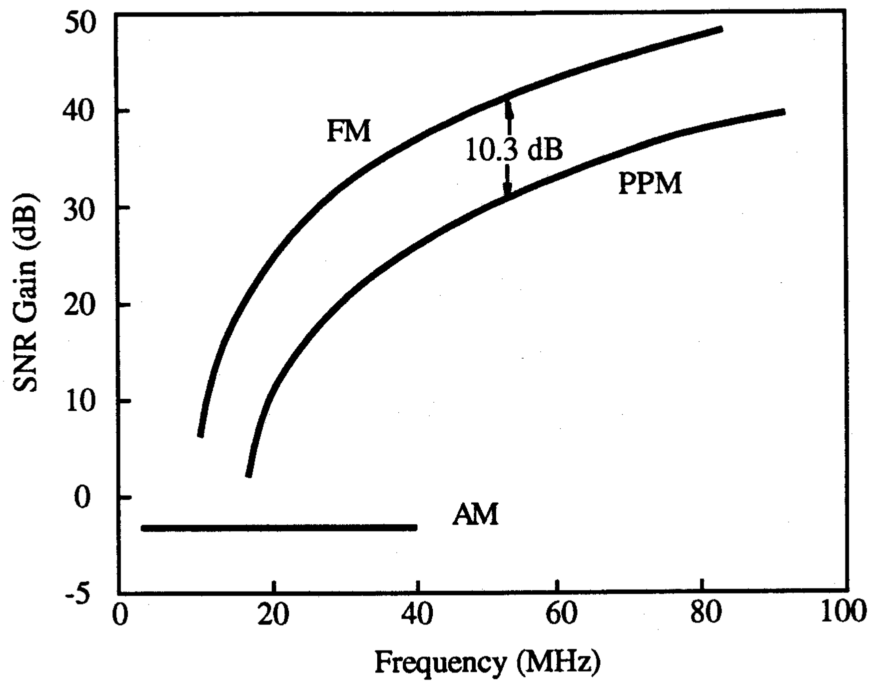

Figure 5.7: SNR gain vs transmission bandwidth spreading.

improvement of over 50 dB is theoretically possible with PPM for a 136.7 MHz bandwidth. Table 5.1 shows that a multichannel PCM scheme needs higher transmission bandwidth than PPM. For a 50-channel system, a total system bandwidth of 5.4 GHz is necessary for PCM, while a comparable PPM system occupies a 3.75 GHz bandwidth.

As discussed in the section on FM SNR, the SNR improvement with transmission bandwidth increase for PPM and PCM is based on a constant CNR. With this assumption, SNR gains for AM-VSB, FM, and PPM are plotted against transmission bandwidth in Figure 5.7. SNR characteristics for FM, PCM, and PPM for an 80 MHz transmission bandwidth are plotted in Figure 5.8. It is seen that the FM format has more improvement than the others for the same transmission bandwidth. Figure 5.7 shows that FM format is about 10.3 dB superior to PPM format over a practical frequency range. FM systems, therefore, are generally preferred for short-haul TV distribution. This bandwidth-SNR

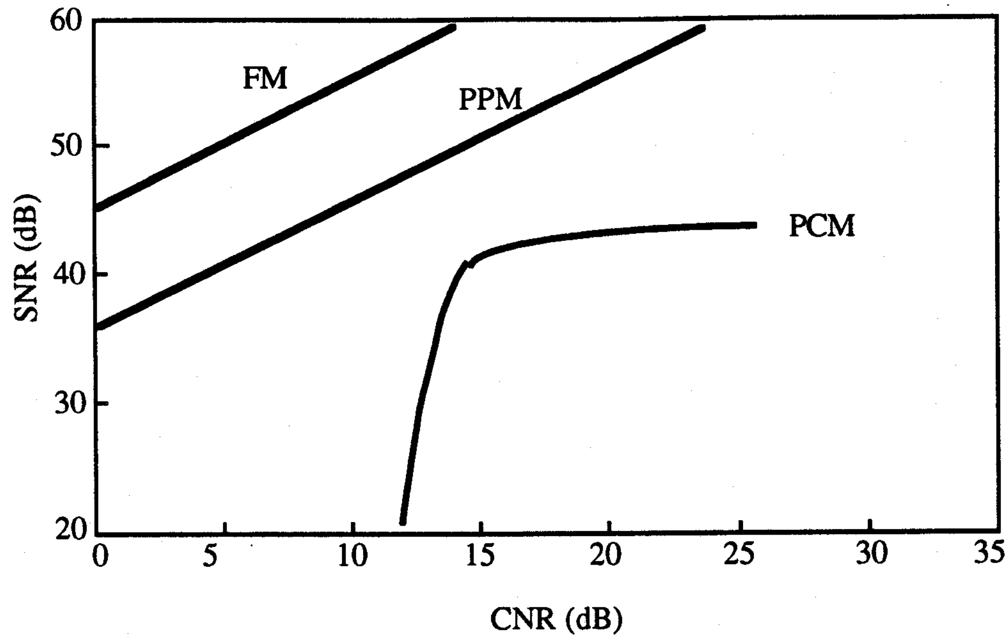

Figure 5.8: SNR improvement for same transmission system bandwidth (B_t = *80 MHz*).

exchange does not occur in AM-VSB systems. The SNR_{AM} is strictly proportional to the input CNR_{AM}. Figure 5.8 shows that SNR_{PPM} for PPM is about 8.5 dB superior to PCM with 6 bits/sample for the same transmission bandwidth.

6. FUNDAMENTAL LIMIT ON NUMBER OF CHANNELS IN LIGHTWAVE VIDEO SYSTEMS

In previous chapters, video signal transmission on a fiber optic link using AM-VSB, FM, PCM, and PPM was compared in terms of signal-to-noise ratio performance. The discussions were based on the assumption that the input/output characteristics of the laser are linear. However, in the design of a fiber optic link for multichannel video transmission using traditional analog AM-VSB and FM formats, it is necessary to consider the fact that the transfer relationship is not exactly linear. Each element in the optical link, such as the laser, the laser driver, the photodiode, and the receiver amplifier, has a nonlinear transfer characteristic. In general, the typical link is dominated by laser nonlinearity.

This chapter will discuss intermodulation distortion and clipping distortion caused by the laser transmitter and the photodiode receiver. These nonlinear impairments limit the usable optical power level and deteriorate the signal-to-noise ratio performance for the AM-VSB and FM fiber optic link. This problem is primarily responsible for the limitation on the number of channels in AM-VSB and FM lightwave video systems.

6.1. Intermodulation Distortion

In Chapter 3, Figure 3.1 shows the light vs current transfer characteristic without distortion above the lasing threshold. As the laser is ramping up and down about a low bias current, there is little distortion at low modulation frequencies. However, it has been

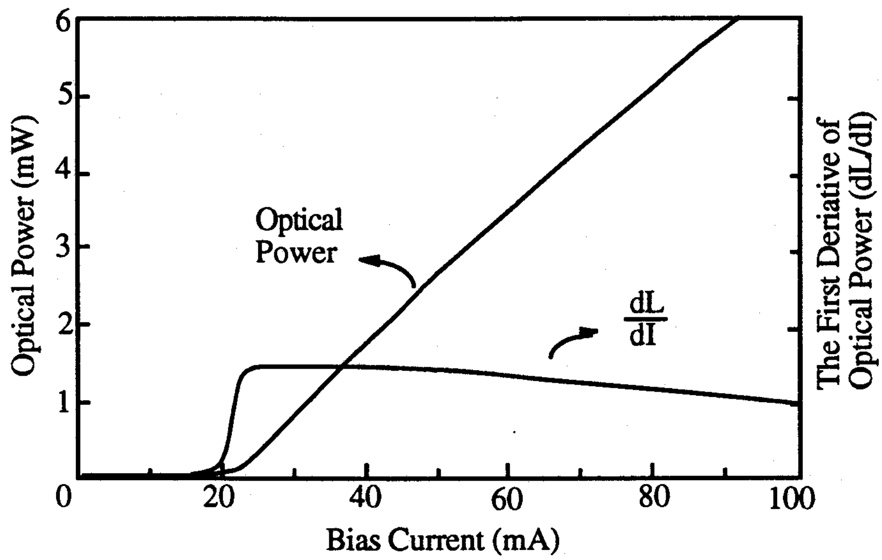

Figure 6.1: Typical light-current of laser with quasi-nonlinear characteristic.

shown that as either the bias current or modulation frequency increases, the nonlinearity distortions increase very rapidly [21]. Figure 6.1 shows a typical nonlinear light-current curve, as well as the first derivative of the output light power with respect to the bias current. The derivative of the characteristic in this figure can graphically provide additional information about the laser. Ideally, $\frac{dL}{dI}$ would be perfectly flat above the lasing threshold, but in all practical lasers, $\frac{dL}{dI}$ decreases at higher driving currents. The deviation from ideal is of interest because it produces the unexpected frequency components called intermodulation distortion at the laser output.

Assume the applied modulation current of a multichannel video signal is:

$$I(t) = I_o + \sum_{i=1}^{N} m_i \cos(2\pi f_i t + \phi_i) \tag{6.1}$$

where I_o is the *dc* bias current, and m_i and ϕ_i are the modulation index and the phase of the *i*th carrier, respectively. Then the light output $L(t)$ from a laser with a quasi-nonlinear characteristic, in response to the modulation, is given by [22]

$$L(t) = L_o + \sum_{n=1}^{\infty} \frac{1}{n!} \left| \frac{d^n L}{dI^n} \right| [I(t) - I_o]^n \tag{6.2}$$

where L_o is the power at the *dc* bias current. Amplitude or frequency modulation is accomplished by varying m_i and f_i, respectively.

Equation 6.2 indicates that the nonlinearity in the transfer characteristic may have a profound effect on the output signal. To see the effect of a multichannel load, it is instructive to consider an input of two carriers at frequencies f_1 and f_2. The output then contains not only the desired first-order term changed in amplitude, but also it is accompanied by terms at *dc*, second, third, and higher order components of the fundamental input frequency. These spurious-frequency components are called modulation products. In practice, only the terms at second- and third-order frequencies are of interest since $\frac{d^n L}{dI^n}$ is negligible for n greater than 3.

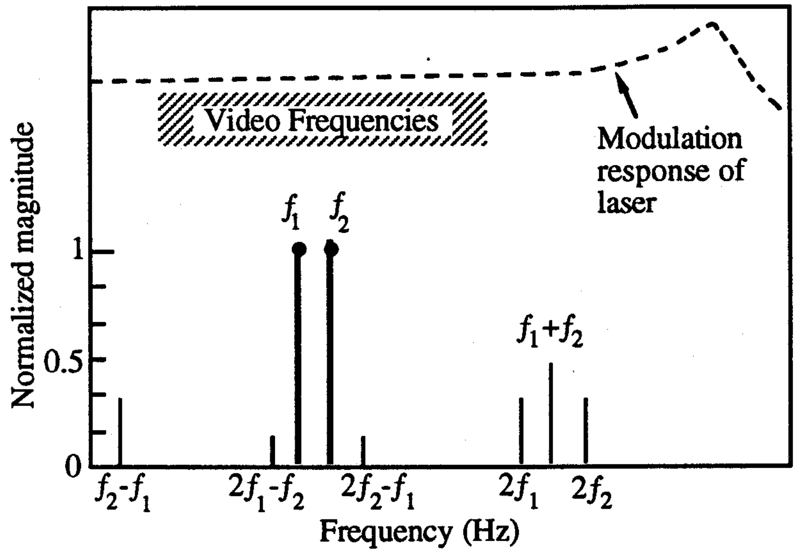

Figure 6.2: Two carriers and their modulation products.

The modulation products arising from the two-frequency inputs are shown in Figure 6.2. It can be seen from this figure that the third order products at frequencies $2f_1 - f_2$ and $2f_2 - f_1$ are most likely to lie within the standard video frequency band. However, for a large number of channels, both second and third order distortions will lie within the frequency range to be used. Figure 6.3 (a) and (b) show the distribution of second- and third-order distortion products , respectively, produced by a 50-channel load.

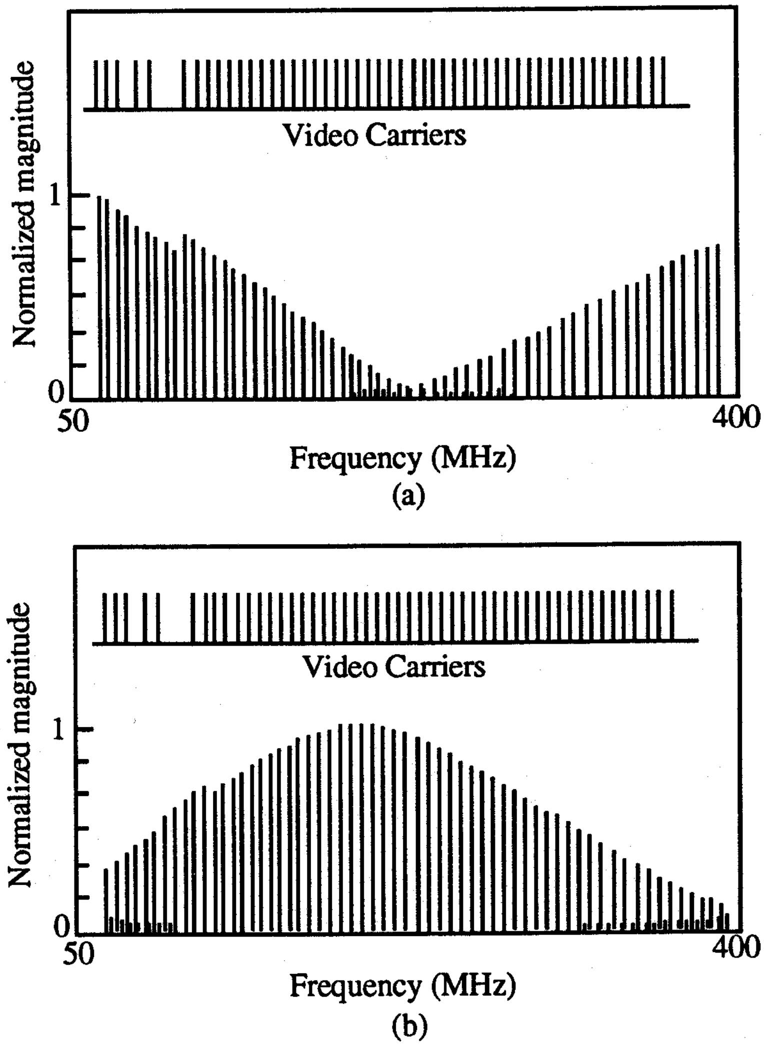

Figure 6.3: The intermodulation distortion distribution: (a) the second-order products and (b) the third-order products.

In actual applications of multichannel video transmission, baseband video signals in different channels are carried on a number of well separated high-frequency carriers. The number of second- and third-order products can be calculated by summing over all possible combinations of channels. Table 6.1 made by Darcie [23] lists the number of second- and third-order products for various channel loads within the standard NTSC frequency band. These numbers are dominated by products of the type $f_i \pm f_j$ and $f_i \pm f_j \pm f_k$, for second and third order, respectively. These counts allow for estimation of the allowable magnitude of each type of products.

Equation (6.2) also indicates that the magnitude of distortion varies with the modulating signals. Figure 6.4 shows the characteristic of second order distortion versus the input bias current. It can be seen from this figure that the distortion is at a minimum at a low bias current, where the second derivative of the light with respect to the bias current, $\frac{d^2L}{dI^2}$, is constant, and the distortion increases at higher bias current with decreasing $\left|\frac{d^2L}{dI^2}\right|$. This effect may cause the fiber optic link to be unuseable at high signal levels.

Table 6.1: Intermodulation product counts.

Channel Number	Channel Freq. (MHz)	Number of Channel (30)	(42)	(60)
Second Order Distortion				
3	61.25	14	26	44
12	199.25	3	7	25
40	319.25	-	12	12
Third Order Distortion				
3	61.25	123	285	663
12	199.25	225	525	1110
40	319.25	-	372	1120

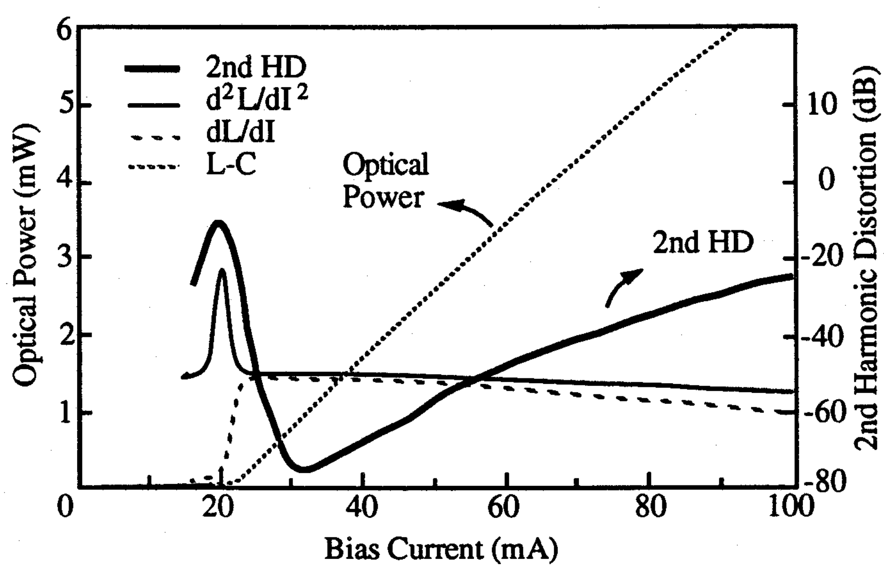

Figure 6.4: The second order distortion vs. bias current.

It has been shown that the magnitude of nonlinear distortion products is not only a function of the bias current, but a function of signal frequencies as well [21]. Second and third order distortions all have maxima at frequencies near one-half laser resonance frequencies, and decrease rapidly with decreasing frequency below the one-half resonance frequency, as shown in Figure 6.5. Although the standard NTSC frequency band does not

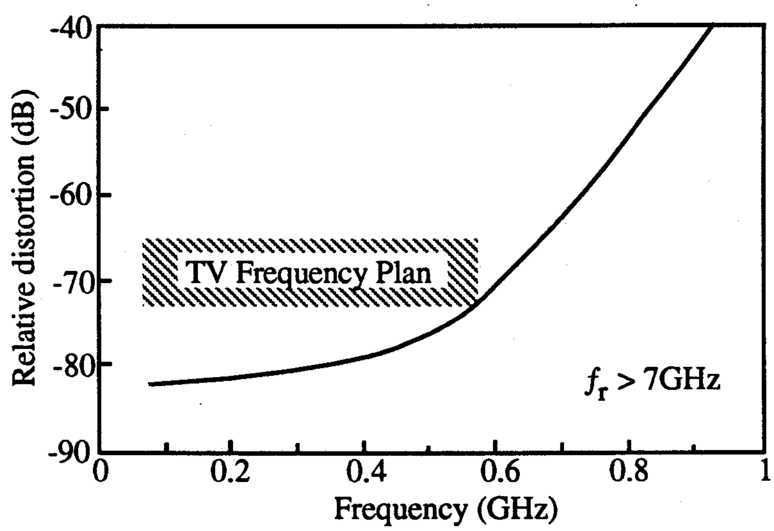

Figure 6.5: Intermodulation distortion vs. frequency.

extend past 550 MHz, laser resonance frequencies greater than about 7 GHz [23] are required to avoid distortion problems. Reducing the resonance frequency shifts the curve in Figure 6.5 to the left, which effectively increases distortion over the band of interest.

Intermodulation distortion can be considered as noise in a multichannel FM system. This will reduce the equivalent SNR performance of FM and make PPM relatively more attractive. This degradation in FM systems will not be analyzed further in this thesis and is left for future work.

6.2. Clipping Distortion

The second type of distortion in the optical video link is called clipping distortion. At a laser transmitter, if the input current level of a multichannel signal exceeds the linear dynamic region of the laser, clipping can occur at zero-power level, as illustrated in Figure 6.6. The linear dynamic region of a commercial high-power lasers is in the range of 125-175 mA, and the corresponding optical output is 100-150 mW [6]. These characteristics of

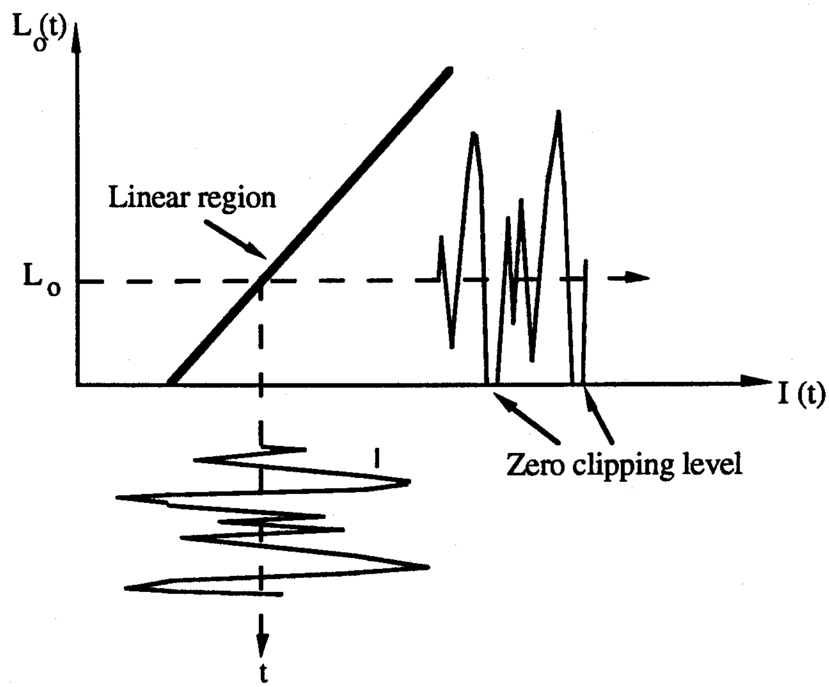

Figure 6.6: Laser clipping distortion.

lasers become the fundamental limitation in multichannel video transmission using analogue AM-VSB or FM.

Assuming that the light vs current transfer characteristic in Figure 6.6 is linear for minimum possible intermodulation distortion, the output optical power in response to the modulation current (Equation 6.1) can be expressed as

$$L(t) = L_0 \left[1 + \sum_{i=1}^{M} m_i \cos(2 \pi f_i t + \phi_i) \right]. \tag{6.3}$$

In this equation m_i is the optical modulation depth, which is defined as the ratio of one-half peak-to-peak amplitude of the modulated optical signal to the optical output from the laser at the *dc* bias level.

It is clear from Equation 6.3 that the output optical waveform $L(t)$ is the sum of M independently modulated sinusoids. Thus, if the optical modulation depth per channel is constrained to $m_i < 1/M$, no signal clipping will occur. However, this restriction limits SNR performance due to the low optical modulation depth allowed in each channel.

For multichannel system implementation, clipping distortion at the receiver must be taken into consideration. The incident optical power at the input of the receiver in a television distortion network will vary from receiver to receiver. This power variation is due to differences in various loss contribution factors from the transmitter to the receiver, such as fiber length and loss, loss in optical coupling, number of connectors and splitters and their total loss, etc. Thus the receiver must operate satisfactorily not only at the minimum incident optical power (for the longest or most lossy link), but also over a range of power levels up to the level determined by the shortest or least lossy link. The maximum allowable optical power level is determined by the nonlinear distortion and saturation characteristics of the receiver.

6.3. Receiver Sensitivity

Both intermodulation distortion and clipping distortion limit the available laser power per channel. The optical power required at the receiver input in order to satisfy the SNR requirements is a measure of the receiver sensitivity. The more sensitive the receiver, the less optical power required. Therefore, one of the goals of receiver design is to maximize sensitivity to allow more video channels transmitted in the optical link.

Recall the equation relating received optical power to electrical current generated by a photodiode:

$$I_{ph}(t) = \frac{q\eta}{h\nu} L(t) = \rho\, L(t).$$

At the output of the photodetector, the received average current of the i^{th} channel from Equation 6.3 is

$$I^2_{ph} = \frac{(\rho\, m_i\, L_o)^2}{2} \tag{6.4}$$

The average electrical signal power per channel delivered by a photodiode to the demodulator with input impedance, R_d, is

$$P_c = \frac{G_a^2 Z_{ph}^2 I_{ph}^2}{R_d} = \frac{1}{2R_d} G_a^2 Z_{ph}^2 \left(\rho m_i\, L_o\right)^2. \tag{6.5}$$

The carrier-to-noise ratio can be calculated as in Chapter 3, where the mean-squared noise voltage for video signal transmission on a fiber optic link was found. The noise power produced by both the laser and the photodetector is

$$P_{nt} = \frac{G_a^2 < V_{nt}^2 >}{R_d} \quad . \tag{6.6}$$

To simplify computations, preamplifier noise and relative intensity noise (RIN) in the laser transmitter are assumed to be negligible. Combining Equation (6.5) and Equation (6.6) yields:

$$CNR \approx \frac{(\rho \; m_i \; L_o)^2}{2\,(<i_{sh}^2> + <i_{th}^2>)} = \frac{(\rho \; m_i \; L_o)^2}{2\left(2\; q\; \rho\; Lo + \frac{4kT}{Rph}\right)B_t} \; . \tag{6.7}$$

Using this result and CNR for PPM in Chapter 3 and CNR for PCM in Chapter 4, CNR objective as a function of power per channel required is shown in Figure 6.7. The bandwidth of each signalling format is 6 MHz for the standard NTSC analog AM-VSB, 40 MHz for analog FM, 75 MHz for PPM, and 108 MHz for digital PCM. A photodiode responsivity of 0.7, modulation depth of 0.1, and equivalent photodiode resistance of 1 kiloohm are assumed for the calculations.

As can be seen in Figure 6.7, the standard NTSC video signal requires a received power of -6 dBm per channel to satisfy its SNR objective of 56 dB as discussed in the

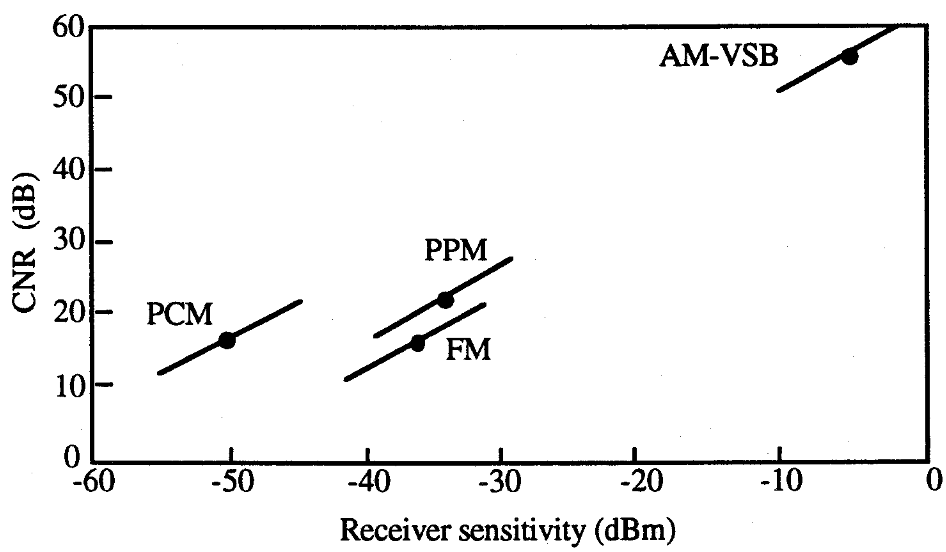

Figure 6.7: The limitation on required power for various signalling formats.

previous chapter. This condition implies a fundamental limit of 4 channels per milliwatt of received optical power. Analog PPM has a CNR requirement of 23.11 dB to meet the SNR objective of 56 dB. The resulting fundamental limit on the required received incident power per channel is only -33.65 dBm, which offers a huge advantage over AM-VSB. Analog PPM shown in Figure 6.7 require higher receiver sensitivity, -33.65 dBm, than analog FM because more noise is introduced through a larger receiver bandwidth. Since, both PCM and PPM signals are transmitted as fixed amplitude pulses, receiver sensitivity is independent of the number of channels loaded in the fiber optic link.

7. INTEGRATED SERVICES USING PPM AND PCM

In television broadcasting, audio signals must be transmitted with video signals to subscribers' TV sets. The audio signals can be transmitted only by pulse modulation techniques (PTM or PCM) if the video signals are transmitted by PPM. Since the baseband audio frequencies are much lower than the baseband video frequencies, it is easy to multiplex the audio signal with the PPM video signal by employing pulse code modulation. With this basic concept, it is possible that the transmission of a PPM video signal can be combined with other information from different sources, such as stereo music, "AM" radio signals, and data. This chapter presents the idea of integrated services using PPM and PCM.

7.1. PPM and PCM Multiplexing System

PPM video signals consist of discrete pulses in which the pulse displacement varies within a specified time slot. It is possible to use other time slots for PCM signals. When PPM and PCM signals are combined together such that they do not overlap in the time domain, it is known as time division multiplexing (TDM).

An integrated service system using PPM and PCM is illustrated in Figure 7.1 (a). The PCM information from these sources can be efficiently accommodated within a single time slot by using an audio/data multiplexer. Then PPM video signals and PCM audio/data signals are integrated by a video multiplexer. The video multiplexer stays at each position for one complete time slot to allow each channel to send its PPM or PCM pulses. At the

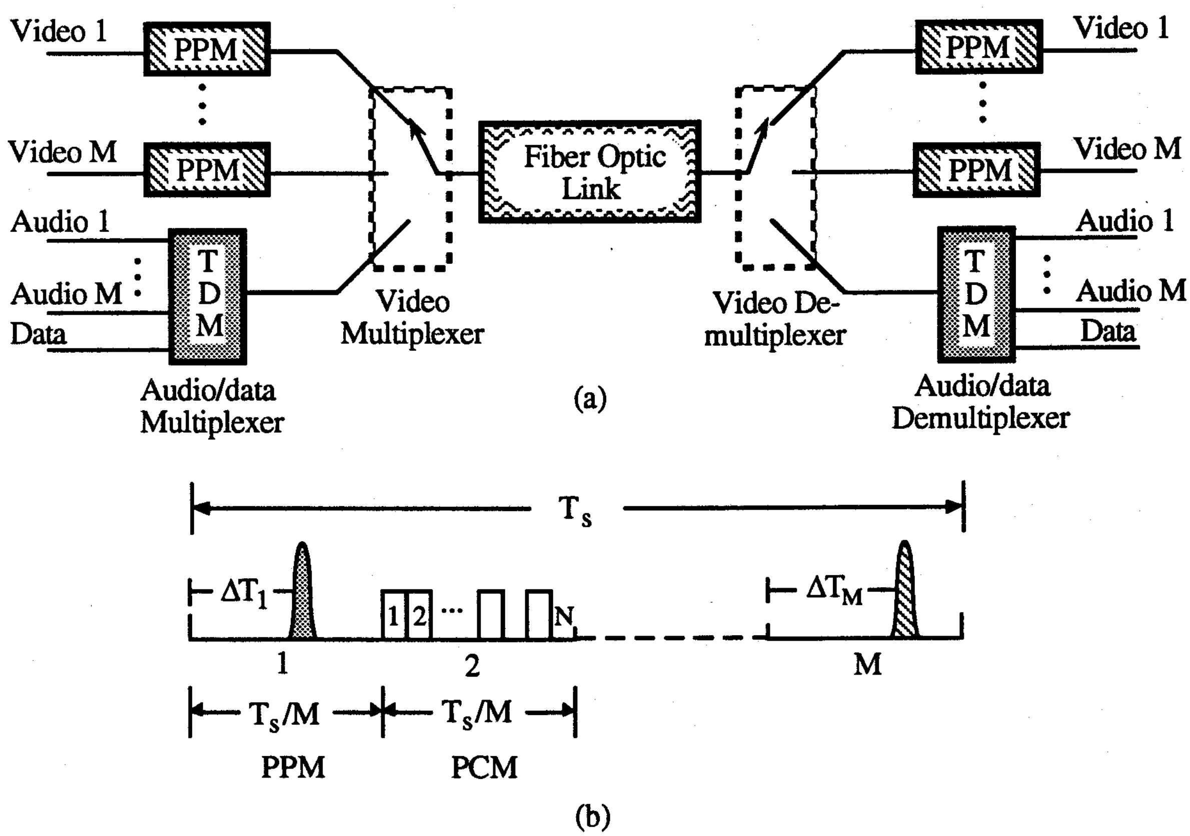

Figure 7.1: Multiplexed PPM and PCM system.

receiver, a multiplexer rotates in synchronization with that at the transmitter in order to divide the multiplexed signals into their respective channels. In practice, this synchronization is not trivial to implement.

In the integrated service system, blocks are consecutively transmitted and the duration of each block is equal to the sampling period used in multiplexed PPM. Each block is divided into M equal time slots. On the transmitting side, one optical PPM pulse is transmitted during one time slot and N binary bits of PCM information are transmitted during another time slot. Figure 7.1 (b) shows an integrated signal block structure.

7.2. Transmission Bandwidth Requirement

In designing such a multiplexed PPM and PCM system, it is apparent that all signals to be multiplexed must either be of the same bandwidth, or sampling must take place at a rate determined by the maximum bandwidth signal. The sampling frequency for video signals is, in general, much higher than that for audio signals or data signals. As mentioned in Chapter 2, the transmission bandwidth for PPM video signal is considered as $B_t = 1/\tau_p$. For PCM, if the duration of the time slot is represented as T_s/M, the bandwidth required by an N-bit per sample digital stream is approximately given by

$$B_{PCM} \approx \frac{M}{T_s} N \tag{7.1}$$

where T_s is the video signal sampling period.

To obtain optimal bandwidth utilization, PPM pulse and PCM bit durations should be equal. Therefore, the relationship between PPM pulse width and the number of PCM bits in a time slot is given by

$$\tau_p = \frac{T_s}{MN} \,. \tag{7.2}$$

7.3. Other System Design Considerations

(a) Jitter

In an ideal digital transmission system, the bits in a digital bit stream arrive at times that are integer multiples of the bit period. However, in real systems, bits arrive at times that differ slightly from the ideal times. This unwanted modulation of bit positions in the bit stream is called *jitter*. The primary sources of jitter in digital transmission systems are regenerators and multiplexers.

Jitter is an anomaly that especially affects the design of the multiplexing system for PPM signals since the transmitted information is contained in pulse positions. However, the design of regenerators and multiplexers is beyond the scope of this thesis.

(b) Laser Time Delay

The physical basis of operation for the laser is stimulated radiative transitions from elevated electron energy levels in the conduction band to their reference levels in the valence band. The stimulated radiative transitions cause photons to be emitted. The dynamic and steady-state behavior of the laser can be studied using rate equations. These equations express the densities of excess electrons and photons in terms of the pumping current and laser parameters. Solutions to the rate equations describe the steady-state conditions and the dynamic response of the laser to a disturbance. The steady-state value for photon density is [24]

$$\phi_s = \left(\frac{\tau_{ph}}{qd}\right)(J - J_{th}) \tag{7.3}$$

where τ_{ph} is the life of a photon, q is the charge of an electron, d is the thickness of the recombination region, and J and J_{th} is current density and threshold current density, respectively.

Equation (7.3) shows that there will be some time delay before J reaches J_{th}. In order words, the laser needs time to build up the optical power in a resonator. Figure 7.2

shows that when an electrical pulse is applied to the laser, the optical output pulse appears after a time delay τ_d which may be in the order of a few nanoseconds [25].

In a PPM video system, the time delay may cause overlapping between optical pulses and their adjacent pulses. For this reason, a guard time should be provided between adjacent channel time slots.

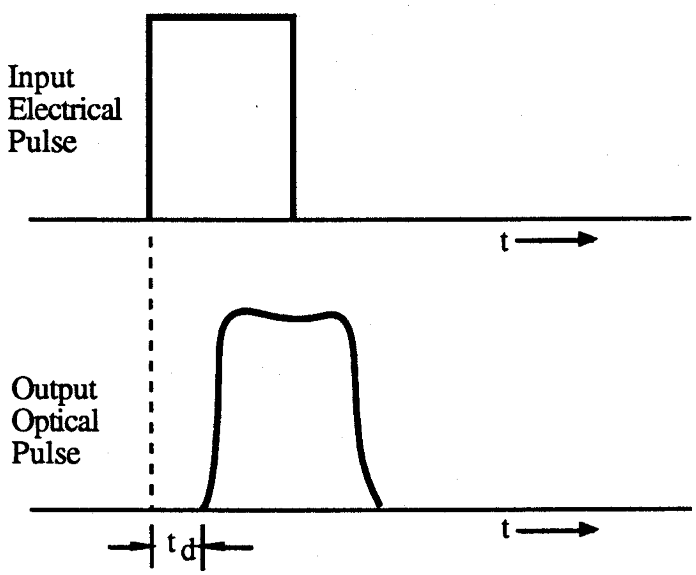

Figure 7.2: The time delay of an output optical pulse.

8. SUMMARY AND CONCLUSION

An investigation in the use of pulse position modulation for video transmission on optical fiber was carried out. The goals of this project were to examine the technical feasibility of PPM on a fiber optic link and to compare its SNR performance with that of other modulation systems. A brief summary of the work in this thesis is presented in this chapter and conclusions from the research work are given.

The evolution of lightwave transmission technology in TV distribution systems provides the opportunity to transmit broadband video over optical fiber. The advantages of optical fiber allow for distribution systems without intermediate repeaters between the television station and subscriber homes. Recent technological advances have led the industry to closely examine the economic and technological feasibility of modulation methods for video transmission on optical fiber links.

AM-VSB is currently used in TV distribution systems over coaxial cable or optical fiber. As discussed in Chapter 2, AM-VSB is very attractive in distribution systems since it is the established modulation for television broadcast transmission. New equipment for AM-VSB transmission over optical fiber can easily connect to existing network facilities. The smooth transition from coaxial to fiber makes AM-VSB the least expensive choice. In addition, AM-VSB is bandwidth efficient, requiring only 6 MHz per channel. The drawbacks are its suitabitity for only shot-haul transmission, and its sensitivity to noise. Laser nonlinearity is the fundamental limitation to the application of this technique for multichannel video transmission. High SNR requirements are difficult to achieved because AM modulation does not improve signal quality over CNR.

Frequency modulation is used in satellite video transmission. Compared to AM-VSM, FM has greater immunity to noise and transmission impairments. Although FM is not very efficient, requiring above 40 MHz per channel, the enormous bandwidth of optical fiber allows high-deviation FM and the subsequent enhancement of SNR performance over CNR. The difficulty with repeaters in AM is also present in FM: loss in signal quality as a result of nonlinear repeaters. However, this is not serious problem because the FM enhancement factor of SNR over CNR allows for greater degradation in transmission quality.

Digital techniques have been used for point-to-point video transmission. The advantages of digital modulation are well known: improved signal quality, longer repeaterless distances, simpler repeaters, etc. However, the digital approach is not always preferable because of the requirement for complex and costly equipment. At present and in the foreseeable future, expensive video codecs diminish the feasibility of the large-scale PCM video distribution to the home.

The purpose of this thesis was to investigate pulse position modulation for multichannel video transmission. PPM utilizes variations in the timing of pulse to convey information about the amplitude of a video signal. Pulse position modulation can be considered more suitable for fiber optic communication than AM or FM, since an optical source is simply turned "on" and "off". The performance of PPM is, hence, largely immune to the effects of nonlinearity in optical transmitters, which degrade analog AM-VSB signals. PPM and PCM signals can be integrated through time division multiplexing for transparent mixing or drop-and-insert of video, audio, and data signals, as described in Chapter 7.

A PPM video transmission system was described in Chapter 3. The SNR performance of PPM video transmission based on a typical noise background was analyzed in Chapter 4. The results shows that PPM SNR improvement comes at the expense of increased transmission bandwidth. For a PPM system operating under typical parameters, a 35.8 dB improvement in SNR performance over CNR can be achieved from 75 MHz of transmission bandwidth. The enormous bandwidth of optical fiber is conducive to high-deviation PPM transmission, improving SNR performance at the expense of bandwidth.

The comparison of PPM SNR characteristics with AM-VSB, FM, and PCM in terms of CNR and bandwidth was studied in Chapter 5. Modulation systems are not equally immune to noise during demodulation. For typical systems, PPM SNR performance is much better than that in AM-VSB close to those in FM and PCM, and can in fact exceed the SNR performance in PCM. The results of SNR analysis for PPM video transmission over optical fiber based on typical background noise show that PPM is acceptable method.

The disadvantages of PPM are lower video channel capacity per fiber, compared to analog AM-VSB and FM. Forthermore, like FM and PCM systems, each receiving site has to demodulate the individual channels to recover their respective AM-VSB video signal for any further distribution.

REFERENCES

1. J. Lipson, L. C. Upadhyayula, S. Huang, C. B. Roxlo, E. J. Flynn, P. M. Nitzsche, C. J. McGrath G. L. Fenderson, and M. S. Schaefer, "High-Fidelity Lightwave Transmission of Multiple AM-VSB NTSC Systems", *IEEE Transactions on Microwave Theory and Techniques*, Vol. 38, No. 5, pp. 483-493, May 1990.

2. R. Olshansky and V. A. Lanzisera, "60-Channel FM Video Subcarrier Multiplexed Optical Communication System", *Electronics Letters*, Vol. 23, No. 22, pp. 1196-1197, October 1987.

3. M. Yamada and S. Nishikawa, "Fiberoptic Digital Video Transmission Systems", *Hitachi Review*, Vol. 37, No. 3, pp. 133-138, May 1988.

4. D. H. Pritchard,"Standards and Recommended Practices", *Television Engineering Handbook*, McGraw-Hill Book Company, NY,1986.

5. D. G. Fink, "Television Fundamentals and Standards", *Electronics Engineers' Handbook*, 3rd Ed., McGraw-Hill Book Company, New York, 1989.

6. C. Lin, "Optoelectronic Technology and Lightwave Communications Systems", Van Nostrand Reinhold, New York, 1989.

7. L. Thompson, R. Pidgeon, and F. Little,"Supertrunking Alternatives in CATV", *The Magazine of Lightwave Communication System*, Vol. 1, No. 1, pp. 26-29, February 1990.

8. V. Di Biase, P. Passeri, and R. Pietroiusti, "Pulse Analog Transmission of TV Signals on Optical Fiber", *Alta Frequenza*, Vol. LVI-N.4, pp. 195-203, June 1987.

9. W. D. Gregg, *Analog and Digital Communication: Concepts, Systems, Applications, and Services in Electrical Dissemination of Aural, Visual, and Data Information*, John Wiley & Sons, New York, 1977.

10. K. Peterman and G. Arnold, "Noise and Distortion Characteristics of Semiconductor Laser in Optical Fiber Communication System", *IEEE Journal of Quantum Electronics*, Vol. QE-18, No. 4, pp. 543-555, April 1982.

11. H. Melchior, H. Jaechel, and R. Welter, "Light Intensity Noise in Gain- and Index Guide Semiconductor Heterojunction Lasers", *Integrated Optics-Physics and Applications*, Plenum, New York, pp. 383-393, 1981.

12. D. E. McCumber, "Intensity Fluctuation in the Output of CW Laser Oscillators", *Physical Review* , Vol. 141, pp. 306-325 Jan. 1966

13. K. Sato, "Intensity Noise of Semiconductor Laser Diodes in Fiber Optic Analog Video Transmission", *IEEE Journal of Quantum Electronics*, Vol. QE19, No. 9, pp. 1380-1383, September 1983.

14. T. M. Straus, "The Relationship Between the NCTA, EIA, and CCIR Definitions of Signal-to-Noise Ratio", *IEEE Transactions on Broadcasting*, Vol. BC-20, No. 3, pp. 36-41, September 1974.

15. J. F. Fisher and R. G. Clapp, "Waveforms and Spectra of Composite Video Signals", *Television Engineering Handbook*, McGraw-Hill Book Company, New York,1986.

16. EIA Standard, "Electrical Performance Standard for Television Relay Facilities (EIA-250-B)", *Electronic Industries Association*, 1976.

17. A.P. Robinson, "The Relationship Between Vision Carrier-to-Noise Ratio and Picture Signal-to-Noise Ratio in a System 1 Television Receiver", *Report BBC RD 1987/23*, BBC, Tadworth UK, pp. 1-15, December 1987.

18. L. Clayton, "FM Television Signal-to-Noise Ratio", *IEEE Transactions on Cable Television*, Vol. CATV-1, No. 1, pp. 25-30, October 1976.

19. F. G. Stremler, *Introduction to Communication Systems*, Addison-Wesley Publishing Company Inc., New York, 1982.

20. V. Pasquini, C. Cambareri, G. Zambelli, and G. Marchini, "Digital Transmission on Coaxial and Optical Cable of a 140 Mbit/s PCM-TV Signal", *Proceeding of Telecom '87: Mediterranean Electrontechnical Conference: 34th Congress on Electronics*, Joint Conference, pp. 93-96, 1987.

21. K. Stubkjaer and M. Danielsen, "Nonlinearities of GaAlAs Laser-Harmonic Distortion", *IEEE Journal of Quantum Electronics*, Vol. QE-16, No. 5, pp. 531-537, May 1980.

22. T. E. Darcie, J. Lipson, C. B. Roxlo, and C. J. McGrath, "Fiber Optic Devices Technology for Broadband Analog Video Systems", *IEEE The Magazine of Lightwave Communication Systems*, Vol. 1, No. 1, pp. 46-50, February 1990.

23. T. E. Darcie and G. Bodleep, " Lightwave Subcarrier CATV Transmission Systems", *IEEE Transaction on Microwave Theory and Techniques*, Vol. 38, No. 5, pp. 524-533, May 1990.

24 W. B. Jones, Jr., *Introduction to Optical Fiber Communication Systems*, Holt, Rinehart and Winston, Inc., New York, 1988.

25. P. Neusy and W. F. McGee, "Effects of Laser Nonlinearities on TV Distribution Using Subcarrier Multiplexing", *Canadian Conference on Electrical and Computer Engineering*, Montreal, pp. 833-836, September 1989.

26. D. E. Dodds, S. Kumar, and Y. Ding, "Pulse Position Modulation for Distribution of TV Signals on Optical Fiber", *Canadian Coference on Electrical and Computer Engineering*, Ottawa, September 1990.

27. B. P. Lathi, *Modern Digital and Analog Communication Systems*, Holt, Rinehart and Winston, New York, 1983.

APPENDIX A. SNR OF AM-VSB VIDEO SIGNALS

A.1. Definition of CNR and SNR

A block diagram of an AM-VSB demodulator is shown in Figure A.1. The carrier-to-noise ratio (CNR) may be thought of as being measured at the input of the receiver. The the carrier power P_c is defined as the mean power of the carrier during the synchronizing pulse, while the input noise is defined as equivalent noise emerged from the output of the bandlimiting filter. The signal-to-noise ratio (SNR) is measured on the video waveform. It is defined as the peak-to-peak luminance signal level V_{pp} to the r.m.s. noise level V_n [16].

A.2. Relationship Between Carrier Power and Peak-to-peak Luminance Level

The standard levels of the modulated vision carrier are shown in Figure 5.3. The relationship between the carrier power and voltage after the filter may be simply expressed as:

$$V_c = \sqrt{P_c R_d} \tag{A.1}$$

where R_d is the equivalent impedance of the demodulator.

From inspection of Figure 5.3, during the active line, the carrier component has an amplitude of 62.5% of the peak synchronization pulse and the two sideband components each have an amplitude of 15.6%. Since the filter response is skewed symmetrically in the

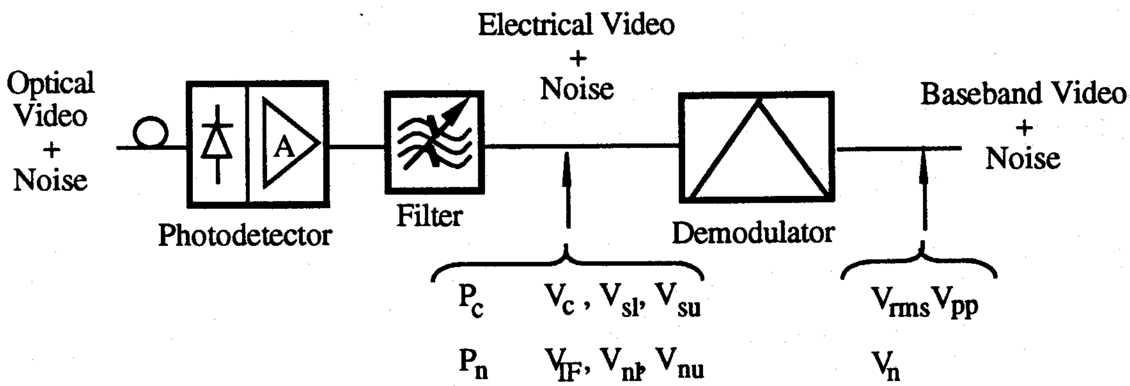

Figure A.1: Block diagram of an AM-VSB receiver.

vicinity of the visual carrier frequency (see Figure 5.2), the upper sideband amplitude after the filter is

$$V_{su} = 0.156\,(1+\Delta)V_c = 0.156\,(1+\Delta)\sqrt{P_c\,R_d} \tag{A.2}$$

Similarly, the lower sideband amplitude is

$$V_{sl} = 0.156\,(1-\Delta)\sqrt{P_c\,R_d} \tag{A.3}$$

where Δ is a small quantity representing the amount of skew.

The amplitudes of coherent sidebands add in the demodulator, producing a baseband video level of

$$V_{rms} = G_m\,(V_{su} + V_{sl}) = 0.156\,G_m\,(1+\Delta+1-\Delta)\sqrt{P_c\,R_d} \tag{A.4}$$

where G_m is the gain of the demodulator.

Hence the peak-to-peak luminance signal voltage is

$$V_{pp} = 2\sqrt{2}\,G_m\,V_{rms} = 2\sqrt{2}\;0.312\,G_m\sqrt{P_c\,R_d} \tag{A.5}$$

A.3. Relationship Between RF Noise Level and Baseband Noise Voltage

The noise voltage after the filter can be related to the RF noise density as follows

$$P_n = N_o B_n \tag{A.6}$$

$$V_{IF} = \sqrt{P_n R_d} \tag{A.7}$$

The noise power after the filter is split between the upper sideband and the lower sideband. The noise voltage in the two sidebands, then, is related to the total noise as

$$V_{IF}^2 = V_{nl}^2 + V_{nu}^2 \tag{A.8}$$

After the demodulator, the two sidebands give baseband noise voltages which are $G_m V_{nl}$ and $G_m V_{nu}$ respectively. The two contributions are incoherent so they undergo power addition, thus the total baseband noise voltage is given by

$$V_n^2 = (G_m V_{nl})^2 + (G_m V_{nu})^2 \tag{A.9}$$

Hence

$$V_n = G_m V_{IF} = G_m \sqrt{P_n R_d} \tag{A.10}$$

A.4. Relationship Between $\mathbf{CNR_{AM}}$ and $\mathbf{SNR_{AM}}$

From the definition, the CNR_{AM} is

$$CNR_{AM} = \frac{P_c}{P_n} \tag{A.11}$$

The definition of SNR gives

$$SNR_{AM} = \frac{V_{pp}^2}{V_n^2} \tag{A.12}$$

Combining the two ratios yields

$$SNR_{AM} = \frac{2\sqrt{2}\ \ 0.312\ G_m \sqrt{P_c\ R_d}}{G_m \sqrt{P_n\ R_d}}$$

$$= 0.625\sqrt{2}\sqrt{\frac{P_c}{P_n}} \tag{A.13}$$

or in decibels

$$SNR_{AM}\ (dB) = CNR_{AM}\ (dB) + 20\ log_{10}\left(0.625\sqrt{2}\right)$$

$$= CNR_{AM}\ (dB) - 1.1\ dB \tag{A.14}$$

APPENDIX B. SNR OF FM VIDEO SIGNALS

B.1. Definition of CNR and SNR

The carrier-to-noise ratio (CNR) is measured at the input of a discriminator shown in Figure B.1. The carrier power P_c is defined as the power of the carrier frequency. The noise is defined as total noise measured at the output of the bandlimiting filter. The FM signal-to-noise ratio (SNR) is defined as the peak-to-peak luminance signal level V_{pp} to the r.m.s. noise level V_n.

B.2. The Video Signal at the Demodulator Output

An ideal frequency-modulation discriminator is a device whose output voltage is linearly proportional to the frequency of a waveform applied to it:

$$V_{out} = k_d\,(f_i - f_o) \tag{B.1}$$

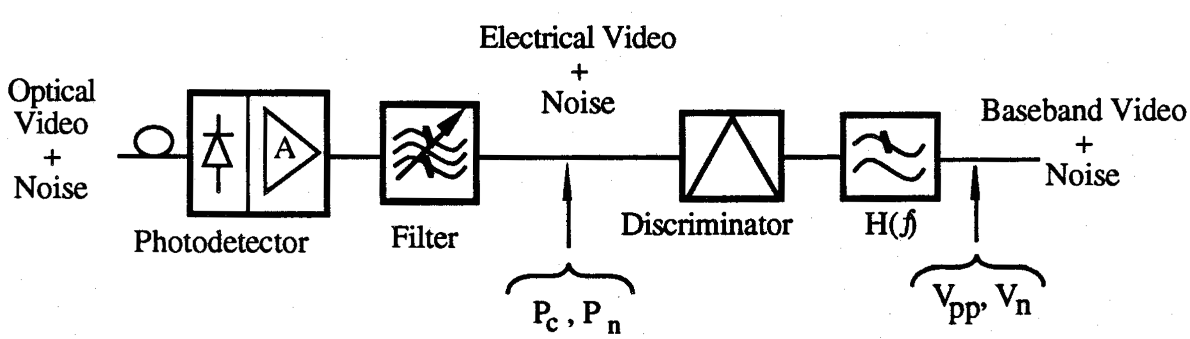

Figure B.1: Block diagram of a FM receiver.

where k_d is the constant of proportionality, f_i is the input waveform frequency, f_o is center frequency.

By EIA-RS-250-B standard [16], if the peak-to-peak deviation ΔF_{max} is produced by the amplitude between the white reference level and the top of the synchronization pulse, the peak-to-peak luminance signal voltage out of the discriminator is

$$V_{pp} = 0.714\ k_d\ \Delta F_{max}\ . \tag{B.2}$$

B.3. The Noise Power at the Demodulator Output

Assuming a tiny sinusoid with rms amplitude due to optical link noise applied at frequency $f_c + f_n$, the bandpass representation at the discriminator input for the bandlimited carrier can be written as:

$$\begin{aligned} v_v(t) &= v_c(t) + v_n(t) \\ &= \sqrt{2}\, a_c \ \sin(2\pi f_c t) + \sqrt{2}\, a_n \ \sin[2\pi(f_c - f_n)t] \\ &= g(t) \sin[2\pi f_c t + \theta_n(t)] \end{aligned} \tag{B.3}$$

where

$$g(t) = \sqrt{2}\, a_c \sqrt{1 + \left(\frac{a_n}{a_c}\right)^2 + 2\,\frac{a_n}{a_c} \cos(2\pi f_n t)} \tag{B.4}$$

$$\theta_n(t) = \tan^{-1}\left(\frac{\frac{a_n}{a_c} \sin(2\pi f_n t)}{1 + \frac{a_n}{a_c} \cos(2\pi f_n t)}\right). \tag{B.5}$$

The $g(t)$ term is the amplitude modulation and the $\theta_n(t)$ term is the phase modulation. Assuming the noise is small, i.e., that $a_c >> a_n$, Equation (B.5) can be rewritten as

$$\theta_n(t) = \frac{a_n}{a_c} \sin(2\pi f_n t)\ . \tag{B.6}$$

Thus we have a phase modulation that can be expressed as an equivalent frequency modulation

$$v_v(t) = g(t) \sin [2\pi (f_c + \Delta f)t] \tag{B.7}$$

where Δf is obtained from

$$\Delta f = \frac{1}{2\pi}\frac{d}{dt}\theta_n(t) = \frac{a_n}{a_c} f_n \cos (2\pi f_n t). \tag{B.8}$$

For FM, the addition of noise introduces both amplitude noise and phase noise. However, the discriminator is not responsive to amplitude variation. Its output is then

$$\begin{aligned} v_{out}(t) &= k_d (f_c + \Delta f - f_o) \\ &= k_d\left(f_c + \frac{a_n}{a_c} f_n \cos (2\pi f_n t) - f_o\right). \end{aligned} \tag{B.9}$$

The mean squared value of the *ac* part of the voltage due to the noise, averaged over a cycle of f_n is

$$< v_{on}^2 > = \frac{k_d^2}{2}\left(\frac{a_n}{a_c} f_n\right)^2. \tag{B.10}$$

Assuming a_n^2 as equivalent sinusoid representing the noise power in a frequency slot df_n wide centered on $f_c + f_n$, there are infinitely many such sinusoids. For white noise on the input side with density N_o watts per Hertz, they have the equal amplitudes and random phases. Taking a_n^2 to be developed across an arbitrary resistive impedance R,

$$N_o\, df_n = \frac{a_n^2}{R} \tag{B.11}$$

$$a_n^2 = R\, N_o\, df_n. \tag{B.12}$$

The carrier power P_c is developed across the same load

$$P_c = \frac{a_c^2}{R} \tag{B:13}$$

$$\left(\frac{a_n}{a_c}\right)^2 = \frac{N_o}{P_c}\, df_n. \tag{B.14}$$

The total mean-squared noise voltage at the discriminator output due to components within the video baseband is the integral of the mean-squared voltage due to the components in the infinitesimal slots

$$V_n^2 = \int_0^{F_v} 2\, \frac{k_d^2}{2} \frac{N_o}{P_c} f_n^2 \, df_n \tag{B.15}$$

where F_v is the video baseband frequency.

If the discriminator is followed by a deemphasis, bandlimiting filter, and weighting network with transfer function, $H(f_n)$, the total noise voltage, then, becomes

$$V_n^2 = k_d^2 \frac{N_o}{P_c} \int_0^{F_v} f_n^2 \, |H(f_n)|^2 \, df_n. \tag{B.16}$$

We now introduce the concept of the “noise bandwidth" of a filter function. It is the bandwidth of a hypothetical ideal rectangular filter that would admit the same amount of noise power to its output as does a real filter with arbitrary response shape, when flat noise of the same power density is applied to both. If B_n is the noise bandwidth of $H(f_n)$ with respect to triangular noise and the noise power transmitted through the ideal rectangular filter is equal to that transmitted through $H(f_n)$, we have

$$\int_0^{B_n} f_n^2 \, df_n = \int_0^{F_v} f_n^2 \, |H(f_n)|^2 \, df_n \tag{B.17}$$

$$\frac{1}{3} B_n^3 = \int_0^{F_v} f_n^{\ 2} \, |H(f_n)|^{\ 2} \, df_n \tag{B.18}$$

$$B_n = \left[3 \int_0^{F_v} f_n^{\ 2} \, |H(f_n)|^2 \, df_n \right]^{1/3} . \tag{B.19}$$

With this replacement in Equation (B.16)

$$V_n^2 = k_d^2 \, \frac{N_o}{P_c} \frac{B_n^3}{3} . \tag{B.20}$$

B.4. The SNR of FM Video Signals

Assuming $H(f_n)$ is sufficiently transparent to the signal that it does not change the peak-to-peak signal voltage, which is still given by Equation (B.2), then we get

$$SNR_{FM} = \frac{V_{pp}^2}{V_n^2} = 1.53 \, \frac{\Delta F_{max}^2}{B_n^3} \frac{P_c}{N_o} . \tag{B.21}$$

For each individual channel in a multichannel system, the SNR of FM may be rewritten in terms of CNR_{FM} as follow:

$$SNR_{FM} = 1.53 \, \frac{\Delta F_{max}^2}{B_n^2} \, CNR_{FM} . \tag{B.22}$$